Newsjournal of the Society for Industrial and Applied Mathematics sinews.siam.org

siam news

Volume 57/ Issue 6
July/August 2024

From a Point to a Torus: Unveiling Emergent Dynamics with Higher-order Bifurcations

By Zachary G. Nicolaou and Adilson E. Motter

Bifurcation theory describes qualitative changes in the solutions of dynamical systems as parameters vary. The theory's origins date back to Henri Poincaré, who foresaw the potential for complexity when stable and unstable manifolds intersect transversally [1, 5]. Many other mathematicians have since contributed to the systematic classification of bifurcations [1, 6]. This classification is aided by consideration of the bifurcation's *codimension*, which is the number of parameters that must be varied for the bifurcation to be observable. Only two generic codimension-one bifurcations of fixed points exist for continuous-time dynamics: saddle-node and Andronov-Hopf bifurcations. Likewise, there are three generic codimension-one bifurcations of limit cycles: saddle-node, period-doubling, and torus bifurcations.

Despite longstanding interest in the field, research continues to reveal new bifurcation phenomena. Bifurcations that are associated with higher codimensions, higher-dimensional invariant sets, and global topological changes are prominent research subjects — as is the analysis of higher-order bifurcations, which occur with the vanishing of leading-order terms in a local expansion. Another important line of inquiry concerns system symmetries, which can guarantee conditions that would otherwise be nongeneric and lower the codimension of higher-order bifurcations [4]. Common codimension-one examples include pitchfork and transcritical bifurcations of fixed points — though other important, less-studied cases exist as well. The ongoing classification of these higher-order bifurcations reveals new insights into emergent phenomena, such as self-organized criticality [11] and the formation of localized states [2]. Our recent work analyzes intriguing higher-order bifurcations to understand

See **Bifurcations** *on page 3*

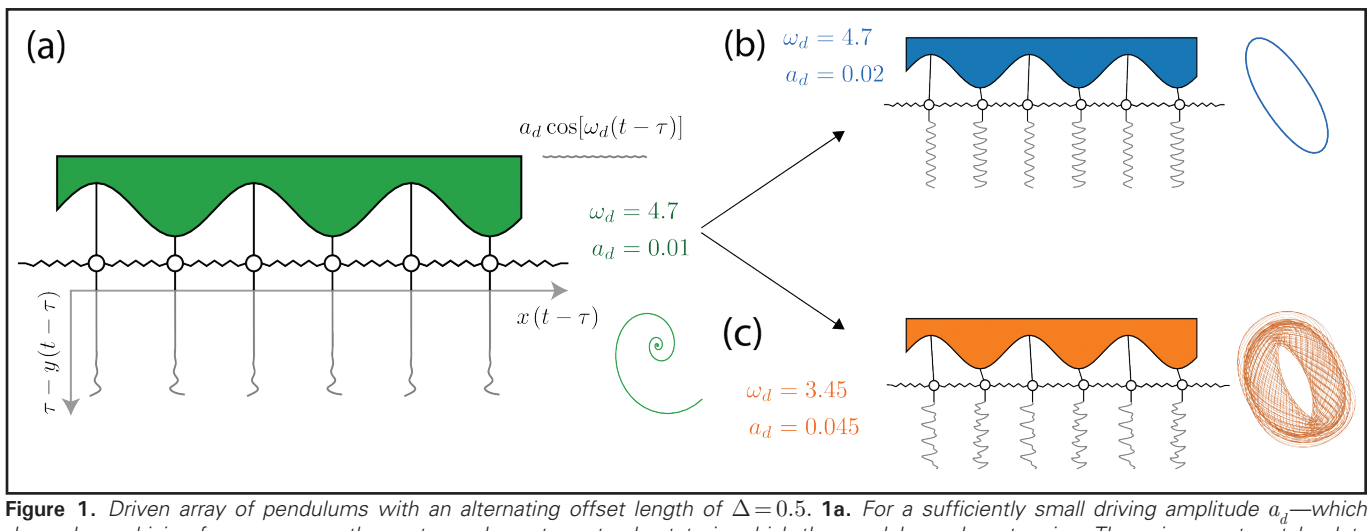

Figure 1. *Driven array of pendulums with an alternating offset length of $\Delta = 0.5$.* **1a.** *For a sufficiently small driving amplitude a_d—which depends on driving frequency ω_d—the system relaxes to a steady state in which the pendulums do not swing. The seismometer-style plots indicate time traces of the pendulum bobs' Cartesian coordinates.* **1b–1c.** *As the control parameter a_d increases, the steady state can bifurcate to either a periodic solution with a subharmonic response (as in* **1b***) or a quasiperiodic solution with an anharmonic response (as in* **1c***), depending on ω_d. The insets depict the corresponding orbits. Figure courtesy of Zachary Nicolaou.*

The Mathematics of Reliable Artificial Intelligence

By Gitta Kutyniok

The recent unprecedented success of foundation models like GPT-4 has heightened the general public's awareness of artificial intelligence (AI) and inspired vivid discussion about its associated possibilities and threats. In March 2023, a group of technology leaders published an open letter[1] that called for a public pause in AI development to allow time for the creation and implementation of shared safety protocols. Policymakers around the world have also responded to rapid advancements in AI technology with various regulatory efforts, including the European Union (EU) AI Act[2] and the Hiroshima AI Process.[3]

One of the current problems—and consequential dangers—of AI technology is its unreliability and subsequent lack of trustworthiness. In recent years, AI-based technologies have often encountered severe issues in terms of safety, security, privacy, and responsibility with respect to fairness and interpretability. Privacy violations, unfair decisions, unexplainable results, and accidents involving self-driving cars are all examples of concerning outcomes.

Overcoming these and other problems while simultaneously fulfilling legal requirements necessitates a deep mathematical understanding. Here, we will explore the mathematics of reliable AI [1] with a particular focus on artificial neural networks: AI's current workhorse. Artificial neural networks are not a new phenomenon; in 1943, Warren McCulloch and Walter Pitts developed preliminary algorithmic approaches to learning by introducing a mathematical model to mimic the functionality of the human brain, which consists of a network of neurons [10]. Their approach inspired the following definition of an artificial neuron:

$$f(x_1,\dots,x_n) = \rho\left(\sum_{j=1}^{n} x_j w_j - b\right),$$

$$f : \mathbb{R}^n \to \mathbb{R},$$

with weights $w_1,\dots,w_n \in \mathbb{R}$, bias $b \in \mathbb{R}$, and activation function $\rho : \mathbb{R} \to \mathbb{R}$, which is typically the rectified linear unit (ReLU) $\rho(x) = \max\{0, x\}$. Arranging these artificial neurons into layers yields the definition of an artificial neural network Φ of depth L:

$$\Phi(x) := T_L \rho(T_{L-1}\rho(\dots(\rho(T_1(x)))\dots)),$$

$$\Phi : \mathbb{R}^n \to \mathbb{R},$$

where $T_k(x) = W_k(x) - b_k$, $k = 1,\dots,L$ are affine-linear functions with W_k as the weight matrices and b_k as the bias vectors. It is worth noting that an artificial neural network is indeed a purely mathematical object.

Let us next discuss the workflow for the application of (artificial) neural networks, which automatically leads to key research directions in the realm of reliability. Given a data set $(x_i, y_i)_i$—which may be sampled from a classification function of data on a manifold $\mathcal{M}$, i.e., $g : \mathcal{M} \to \{1,\dots,K\}$—the key task of a neural network Φ is to approximate the data and the underlying function g. After splitting the data set into a training set and a test set, we can proceed as follows:

(i) Choose an architecture by determining the number of layers in the network, the number of neurons in each layer, and so forth.

(ii) Train the neural network by optimizing the weight matrices and bias vectors. This step is accomplished via stochastic gradient descent, which solves the optimization problem

$$\min_{W_k, b_k} \sum_i \mathcal{L}(\Phi_{W_k, b_k}(x_i), y_i) + \lambda \mathcal{R}(W_k, b_k).$$

See **Artificial Intelligence** *on page 4*

[1] https://futureoflife.org/open-letter/pause-giant-ai-experiments
[2] https://artificialintelligenceact.eu
[3] https://www.soumu.go.jp/hiroshimaaiprocess/en

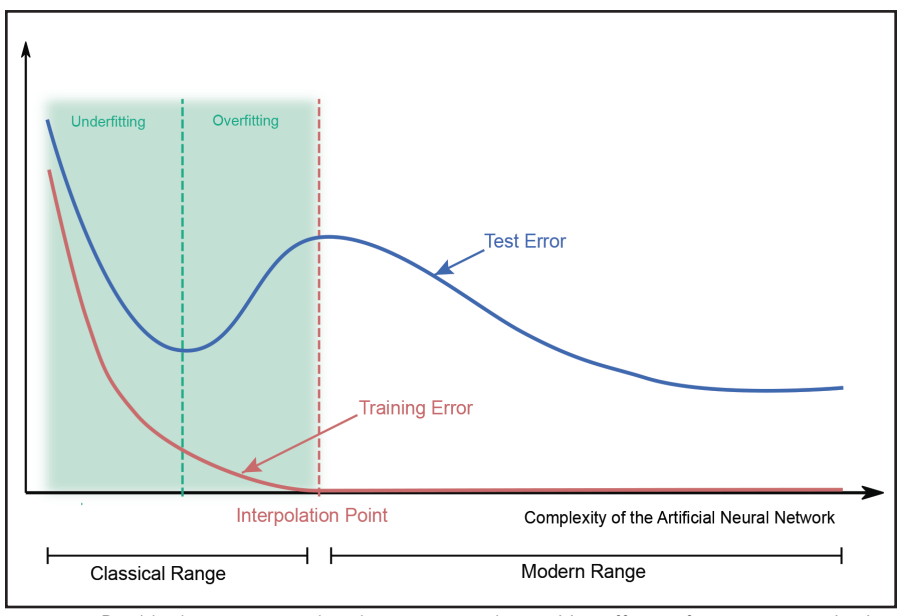

Figure 1. *Double descent curve that demonstrates the positive effects of overparameterization. Figure courtesy of the author.*

siam®
SOCIETY for INDUSTRIAL and APPLIED MATHEMATICS
3600 Market Street, 6th Floor
Philadelphia, PA 19104-2688 USA

siam news
Volume 57/ Issue 6/ July/August 2024

5 **The Importance of Mathematics in Political Decision-making**
Paul Nahin reviews *Mathematics in Politics and Governance*, a new book by Francisco Aragón-Artacho and Miguel Goberna. Through a series of true political stories, historical anecdotes, and college-level mathematical analyses, the authors demonstrate that the disparate worlds of mathematical reasoning and governmental policymaking need not be mutually exclusive.

5 **Does Air Rotate with the Tire?**
Does the air in a rolling tire rotate at the same speed as the tire, assuming that the tire has been rolling with constant speed for some time? Mark Levi explores this question in the context of air flow and drift—acknowledging that the air in the tire is continuously deformed because the lower part of the tire is flattened by the road—and presents a few amusing puzzles.

6 **Modeling the Impact of Rainfall Variability on Vegetation in Drylands**
Given global efforts to adapt to the changing climate and better align mathematical models with the natural timescales of rainfall features and their effects on vegetation patterns, Mary Silber, Punit Gandhi, and Lily Liu build upon an existing fast-slow switching model that contains fast hydrological processes and slow biomass dynamics. Lakshmi Chandrasekaran reports on this research.

8 **LS24 Panel Overviews Industry and Government Career Prospects in the Life Sciences**
During the 2024 SIAM Conference on the Life Sciences—which took place this June in Portland, Ore.—a panel of five researchers from industry and national laboratories reflected on their personal career trajectories, commented on the necessary background knowledge and skillsets for life science projects, and offered advice to junior scientists who are seeking employment in the field.

The Geometry of the Neuromanifold

By Kathlén Kohn

Machine learning with neural networks works quite well for a variety of applications, even though the underlying optimization problems are highly nonconvex. Yet despite researchers' attempts to understand this peculiar phenomenon, a complete explanation does not yet exist. A comprehensive theory will require interdisciplinary insights from all areas of mathematics. In particular and at its core, this phenomenon is governed by geometry and its interplay with optimization [2].

The *neuromanifold* is a key player in the optimization problem of training a neural network. A fixed neural network architecture parametrizes a set of functions, wherein each choice of parameters gives rise to an individual function. This set of functions is the neuromanifold of the network. For instance, the neuromanifold in Figure 1 is the set of all linear maps $\mathbb{R}^3 \to \mathbb{R}^2$ with rank at most one. The neuromanifold in this simple example is a well-studied algebraic variety, but it suggests several tough questions for real-life networks: What is the geometry of the neuromanifold? What does it look like? And how does the geometry affect the training of the network?

Let us explore another simple example of geometry's ability to govern optimization. Imagine the neuromanifold as a full-dimensional subset of $\mathbb{R}^n$ that is closed in the usual Euclidean topology (see Figure 2a). In a supervised learning setting, we provide some training data that is represented as a point in the ambient space $\mathbb{R}^n$. Independent of the choice of loss function to be minimized, only two scenarios can occur during network training: (i) If the data point is inside the neuromanifold, then that point is the global minimum; or (ii) if the data point is outside of the neuromanifold, then the global minimum lies on the neuromanifold's boundary. These scenarios have practical consequences. If we can test a point's membership in the neuromanifold, we can hence reduce the number of optimization parameters by constructing a smaller network that only parametrizes the *boundary* of the original neuromanifold.

This behavior changes drastically when the neuromanifold is a lower-dimensional subset of its ambient space $\mathbb{R}^n$. Suppose that the neuromanifold is a closed, two-dimensional disk inside $\mathbb{R}^3$, and the loss function we want to minimize is the standard Euclidean distance from a given data point. In this case, the global minimum for data points inside the cylinder over the disk will be in the (relative) interior of the neuromanifold, while the minimum for all other points will fall on the (relative) boundary (see Figure 2b). When we alter the loss function, the cylinder changes its shape — which can be challenging to understand.

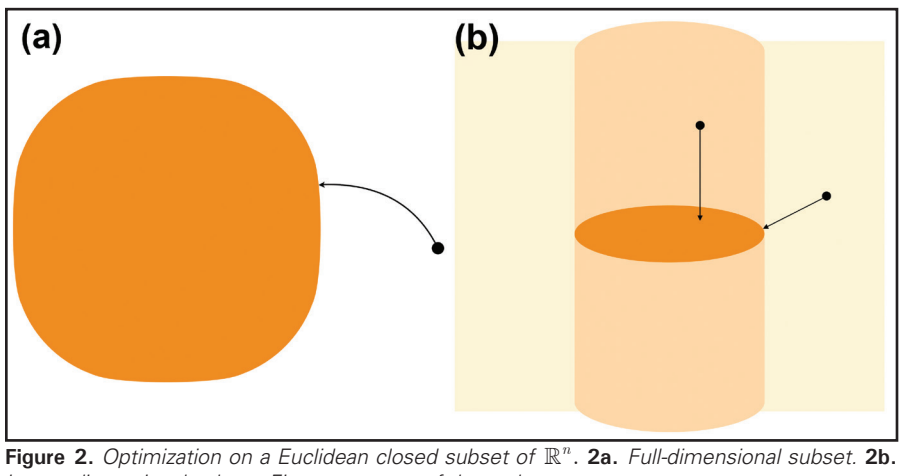

Figure 2. *Optimization on a Euclidean closed subset of $\mathbb{R}^n$.* **2a.** *Full-dimensional subset.* **2b.** *Lower-dimensional subset. Figure courtesy of the author.*

The boundary points of the neuromanifold are not the only interesting points that can become more exposed during training. A neuromanifold often has *singularities*: points at which it does not look locally like a regular manifold. For instance, imagine the neuromanifold as the plane curve in Figure 3 (on page 4), which has one singularity: a cusp. Figure 3 illustrates the data points whose global minimum is the cusp during the minimization of the Euclidean distance. This set of data points has a positive measure, which means that the cusp is the global minimum with positive probability over the data. On the contrary, any other fixed nonsingular point on the curve is the minimum with probability zero.

Of course, the neuromanifolds of actual neural networks are more complicated than these toy examples. Their boundary points and singularities are difficult to describe, but—as in the previous examples—they are important for understanding neural network training. In the context of these optimization properties, an additional layer of complexity arises because the network training does not occur in the space of functions where the neuromanifold lives, but rather in the space of the parameters. Different networks can yield the same neuromanifold, but they parametrize that neuromanifold in distinct ways. Such parametrization often induces spurious critical points in parameter space that do not serve as critical points on the neuromanifold in function space [7].

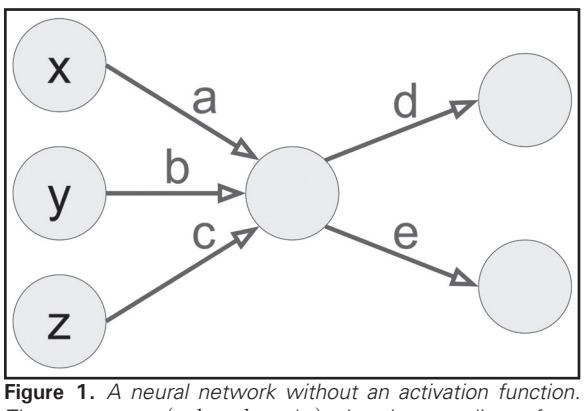

Figure 1. *A neural network without an activation function. The parameters $(a, b, c, d,$ and $e)$ give rise to a linear function $\mathbb{R}^3 \to \mathbb{R}^2$ of rank one, namely $(x, y, z) \mapsto (d(ax + by + cz), e(ax + by + cz))$. Figure courtesy of the author.*

Among the easiest network architectures to study are *fully connected linear networks*. This architecture has no activation function, and all neurons from one layer are connected to all neurons in the next layer. As in Figure 1, the neuromanifold of such a network is an algebraic variety (i.e., a solution set of polynomial equations) that consists of low-rank matrices. Though it has no boundary points, it does have singularities (i.e., matrices of even lower rank). Depending on the loss function, these singularities can be critical points with positive probability (see Figure 3, on page 4). Along with the spurious critical points in parameter space, they play a crucial role in the analysis of the convergence of gradient descent [5].

In a *linear convolutional network*, not all neurons between neighboring layers are connected, and several edges between neurons share the same parameter. More concretely, this type of network parametrizes linear convolutions that themselves are composed of many individual convolutions: one for each network layer. For instance, a linear convolution on one-dimensional signals is a linear map wherein each coordinate function takes the inner product of a fixed filter vector with part of the input vector (see Figure 4, on page 4). The composition of such convolutions in a neural network is equivalent to the multiplication of certain sparse polynomials. And unlike the fully connected case, this network's neuromanifold is typically not an algebraic variety. Instead, it is a semi-algebraic set — i.e., the solution set of polynomial equations and polynomial inequalities (like the disk in Figure 2b) [3]. Moreover, the neuromanifold is closed in the standard Euclidean topology. It typically has a nonempty (relative) boundary whose relevance for network training depends on the network architecture, and particularly on the *strides* of the individual layers.

The stride of a linear convolution on one-dimensional signals measures the speed at which the filter moves through the input vector. If the linear convolutions in all network layers have *stride one*, the neuromanifold is a full-dimensional subset of an ambient vector space with no singularities (see Figure 2a). Its boundary points often manifest as critical points, and spurious critical points also frequently appear [3].

If the linear convolutions in all network layers have *strides that are strictly larger than one*, the dimension of the neuromanifold is smaller than the dimension of the smallest vector space that contains it [4]. The neuromanifold typically has both singularities and boundary points, but—in contrast to all of the other network architectures that we described—they almost never appear as critical points when we train the network via squared error loss (under mild assumptions). More concretely, in the presence of a sufficient amount of generic (i.e., slightly noisy) data, all nonzero critical points of the squared error loss are nonsingular points in the (relative) interior of the neuromanifold [4].

In addition, no nonzero spurious critical points are present in parameter space, which allows us to describe and count all critical points via algebraic methods in function space [6]. Ultimately, the behavior

See **Neuromanifold** *on page 4*

siam news

ISSN 1557–9573. To be published 10 times in 2024: January/February, March, April, May, June, July/August, September, October, November, and December.
The material published herein is not endorsed by SIAM, nor is it intended to reflect SIAM's opinion. The editors reserve the right to select and edit all material submitted for publication.

Advertisers: For display advertising rates and information, contact the Department of Marketing & Communications at marketing@siam.org.

One-year subscription (nonmembers): Electronic-only subscription is free. $73.00 subscription rate worldwide for print copies. SIAM members and subscribers should allow eight weeks for an address change to be effected. Change of address notice should include old and new addresses with zip codes. Please request an address change only if it will last six months or more.

Bifurcations

Continued from page 1

novel symmetry phenomena in networks of coupled oscillators [7-10].

The bifurcations in a vibration-driven array of pendulums with alternating lengths serve as one such example (see Figure 1, on page 1) [8, 10]. The dynamics of this system are governed by

$$\ddot{\theta}_i = -0.1\dot{\theta}_i - \frac{1+(-1)^i 4\Delta + a_d\omega_d^2\cos(\omega_d t)}{1-(-1)^i\Delta}\sin(\theta_i) + \frac{1+(-1)^i\Delta}{1-(-1)^i\Delta}[\sin(\theta_{i+1}-\theta_i)+\sin(\theta_{i-1}-\theta_i)], \quad (1)$$

where θ_i is the angle of the ith pendulum with respect to the vertical direction, a_d is the driving amplitude, ω_d is the driving frequency, and Δ is the alternating offset length. The attracting state for a small driving amplitude corresponds to all pendulums in the vertical position (see Figure 1a, on page 1). This steady state's stability is determined by the Floquet multipliers of the stroboscopic map between consecutive driving periods. For an increasing driving amplitude a_d, one might expect (based on previous studies of Faraday waves) that the pendulums will respond in a subharmonic fashion and oscillate at half the driving frequency, ultimately forming a limit cycle. Such a response does indeed occur for a range of driving frequencies (see Figure 1b, on page 1). However, for other driving frequencies, the first bifurcation that the system encounters is a *direct* transition from a fixed point to an invariant torus (see Figure 1c, on page 1) [10]. We can interpret the latter as a continuous form of a Neimark-Sacker bifurcation, not to be confused with the torus bifurcation (i.e., the torus' emergence from a limit cycle). For the system in (1), this counterintuitive bifurcation yields an anharmonic response in which the pendulums oscillate at frequencies that are incommensurate with the driving frequency ω_d.[1]

From a symmetry perspective, the alternating structure of the pendulum lengths partially breaks the translational symmetry, which manifests as a band gap in the dispersion relation between the wave modes' frequencies and the wavelengths for the corresponding undriven system. The anharmonic response occurs precisely when the system is driven at frequencies within this band gap [10], which suppresses the usual subharmonic response. The underlying mechanism is a *coresonance*—wherein two wave modes mix in order to resonate with the driving frequency—that happens when the frequencies of the wave modes differ by an integer multiple of the driving frequency. Since this condition is typically satisfied when the individual wave mode frequencies are incommensurate with the driving, it provides a simple criterion for the driving frequencies — leading to the anharmonic response and the corresponding response frequencies. We can use this criterion to continuously tune the response frequencies by varying the driving frequency. Another consequence of band gaps is the formation of localized states[2] (gap solitons), which arise from secondary bifurcations that themselves emerge from subcritical primary instabilities [8]. These secondary bifurcations in the pendulum array—which are pitchfork and transcritical bifurcations—lead to both subharmonic and anharmonic gap solitons (see Figure 2) [7]. The soliton solutions are connected by a complicated tangle of bifurcations that appear to exhibit a fractal structure that depends on the system symmetry.

Recent studies have also emphasized the appearance of novel global bifurcations in systems with symmetries that involve time reversal. For instance, homoclinic orbits are structurally unstable in generic damped-driven systems [6], but they can persist under one-parameter variations in autonomous Hamiltonian systems — which are invariant under time reversal. This phenomenon gives rise to the well-characterized branches of localized steady states in the cubic-quintic Swift-Hohenberg equation that emanate from a Hamiltonian-Hopf bifurcation point [2]. Only recently has the community broadly appreciated the presence of other time-related symmetries in dissipative systems as well, such as parity-time (PT) symmetries in non-Hermitian quantum systems [3]. These symmetries constrain the eigenvalues of invariant fixed points (and the Floquet multipliers of invariant limit cycles) so that they are either imaginary or appear in pairs with opposite real parts. Bifurcation points in such systems can thus correspond to *exceptional points*, where eigenvectors coalesce as two or more eigenvalues come together on the imaginary axis.

We recently identified related bifurcation phenomena that are governed by PT symmetries in the rings of Janus oscillators [7, 9]. The Janus oscillators are comprised of pairs of detuned Kuramoto oscillators and defined as $\dot{\theta}_i = \nu_i/2 + \beta\sin(\theta_{i+\nu_i}-\theta_i) + \sigma\sin(\theta_{i-\nu_i}-\theta_i)$, where β and σ are coupling constants and $\nu_i = (-1)^i$; an interactive interface that explores the dynamics of Janus oscillator networks is available online.[3] The rotationally symmetric ring of Janus oscillators exhibits a surprisingly large number of *chimera states*: patterns of coexisting synchrony and asynchrony [9]. It also exhibits a synchronous state wherein the even and odd oscillators form phase-locked groups that appear via a higher-order bifurcation (see Figure 3a). This bifurcation involves a time-reversal invariant limit cycle whose Floquet multipliers are *all* neutrally stable [7]. Consequently, multiple unstable steady states emerge from this higher-order bifurcation point. For larger coupling constants, the unstable steady states undergo global bifurcations of heteroclinic cycles (see Figure 3b) that yield the aforementioned chimera states.

More than a century has passed since researchers first attempted to classify bifurcations. During this time, we have seen considerable progress in both the classification of generic bifurcations with low codimension and the recognition of universality as dictated by system symmetry. Advancements have also connected bifurcations with dynamical phenomena in network systems. These efforts will certainly find important applications as researchers continue to strive for greater control of complex systems.

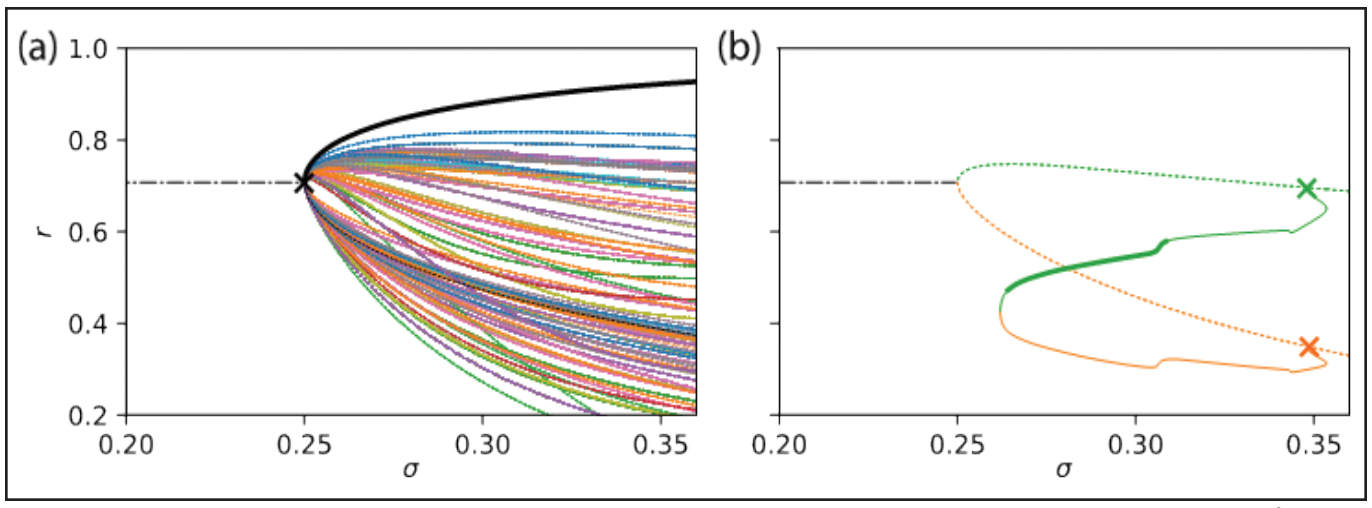

Figure 3. *Bifurcations in the Janus oscillator model.* **3a.** *Kuramoto order parameter r as a function of the coupling parameter σ for $\beta=\sigma$. The solid black line indicates the stable synchronized steady state, the colored lines indicate the unstable steady states, and the dash-dotted line indicates the time-reversal invariant limit cycle.* **3b.** *Bifurcations of traveling chimera solutions that emerge from heteroclinic cycles ("x" symbols) and connect a subset of the unstable states from 3a (dotted and dash-dotted lines). The thick and thin solid lines respectively represent stable and unstable chimera states. Figure courtesy of Zachary Nicolaou.*

References

[1] Arnol'd, V.I. (Ed.). (1994). *Dynamical systems V: Bifurcation theory and catastrophe theory*. In *Encyclopaedia of mathematical sciences* (Vol. 5). Berlin, Germany: Springer-Verlag.

[2] Burke, J., & Knobloch, E. (2006). Localized states in the generalized Swift-Hohenberg equation. *Phys. Rev. E*, *73*(5), 056211.

[3] El-Ganainy, R., Makris, K.G., Khajavikhan, M., Musslimani, Z.H., Rotter, S., & Christodoulides, D.N. (2018). Non-Hermitian physics and PT symmetry. *Nat. Phys.*, *14*, 11-19.

[4] Golubitsky, M., Stewart, I., & Schaeffer, D.G. (1988). *Singularities and groups in bifurcation theory* (Vol. 2). New York, NY: Springer.

[5] Holmes, P. (1990). Poincaré, celestial mechanics, dynamical-systems theory and "chaos." *Phys. Rep.*, *193*(3), 137-163.

[6] Kuznetsov, Y.A. (2004). *Elements of applied bifurcation theory* (3rd ed.). In *Applied mathematical science* (Vol. 112). New York, NY: Springer.

[7] Nicolaou, Z.G., & Bramburger, J.J. (2024). Complex localization mechanisms in networks of coupled oscillators: Two case studies. *Chaos*, *34*(1), 013131.

[8] Nicolaou, Z.G., Case, D.J., van der Wee, E.B., Driscoll, M.M., & Motter, A.E. (2021). Heterogeneity-stabilized homogeneous states in driven media. *Nat. Commun.*, *12*, 4486.

[9] Nicolaou, Z.G., Eroğlu, D., & Motter, A.E. (2019). Multifaceted dynamics of Janus oscillator networks. *Phys. Rev. X*, *9*(1), 011017.

[10] Nicolaou, Z.G., & Motter, A.E. (2021). Anharmonic classical time crystals: A coresonance pattern formation mechanism. *Phys. Rev. Res.*, *3*(2), 023106.

[11] Sormunen, S., Gross, T., & Saramäki, J. (2023). Critical drift in a neuro-inspired adaptive network. *Phys. Rev. Lett.*, *130*(18), 188401.

Zachary G. Nicolaou is a Washington Research Foundation Postdoctoral Fellow and an acting instructor in the Department of Applied Mathematics at the University of Washington. Adilson E. Motter is the Charles E. and Emma H. Morrison Professor of Physics and director of the Center for Network Dynamics at Northwestern University, where he is affiliated with the Department of Physics and Astronomy, Department of Engineering Sciences and Applied Mathematics, and Northwestern Institute on Complex Systems.

[1] See the online version of this article for an animation of the bifurcations that lead to the anharmonic response.

[2] See the online version of this article for an animation of these localized states.

[3] https://www.complexity-explorables.org/explorables/janus-bunch

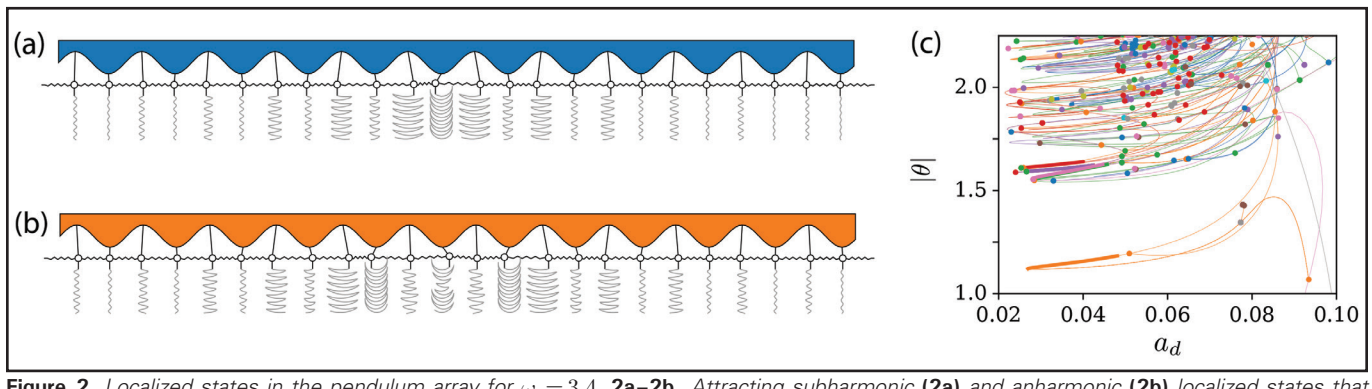

Figure 2. *Localized states in the pendulum array for $\omega_d = 3.4$.* **2a–2b.** *Attracting subharmonic* **(2a)** *and anharmonic* **(2b)** *localized states that emerge from random initial conditions for $a_d = 0.045$.* **2c.** *Bifurcation diagram for the norm $|\theta| = (\Sigma_i \int \theta_i^2 dt)^{1/2}$ versus the driving amplitude a_d, which illustrates the tangle of localized limit cycles that stem from numerical continuation. The thin lines represent unstable limit cycles, the thick lines represent stable limit cycles, and the dots represent higher-order branching bifurcation points. Figure courtesy of Zachary Nicolaou.*

Neuromanifold

Continued from page 2

of critical points for linear convolutional networks with all strides larger than one is more favorable than that of linear networks that are fully connected or convolutional with stride one; this is because the latter networks commonly have nontrivial spurious and singular/boundary critical points, at which gradient descent can get stuck.

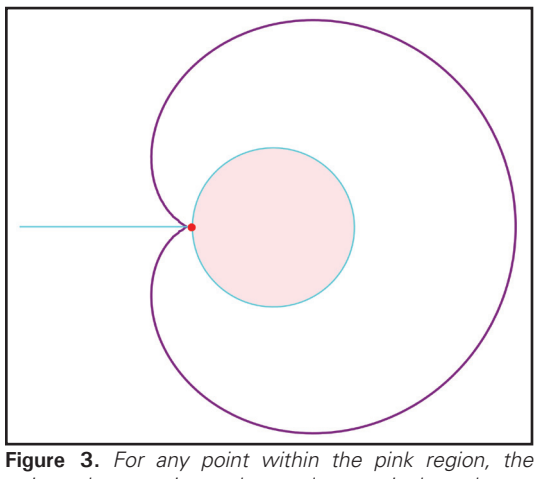

Figure 3. *For any point within the pink region, the unique closest point on the purple curve is the red cusp. In the teal region, the red cusp is one of several closest points. Figure courtesy of [1].*

In conclusion, we can drastically change the geometry of a neuromanifold by varying the architecture of its neural network. For the simple architectures that we describe here, the neuromanifold is a stratified manifold that consists of low-rank matrices/tensors or reducible polynomials. Its geometry governs the optimization behavior during network training. We have demonstrated the impact of replacing fully connected layers with convolutional layers in linear networks; future work will reveal the corresponding effect on nonlinear networks. Interested researchers can use algebro-geometric tools [2] to explore algebraic activation functions, such as the rectified linear unit [8] or polynomial activation. The study of other activation functions will require analytic techniques and collaborations between several mathematical areas.

References

[1] Brandt, M., & Weinstein, M. (2024). Voronoi cells in metric algebraic geometry of plane curves. *Math. Scand.*, *130*(1).

[2] Breiding, P., Kohn, K., & Sturmfels, B. (2024). *Metric algebraic geometry*. In *Oberwolfach seminars* (Vol. 53). Cham, Switzerland: Birkhäuser.

[3] Kohn, K., Merkh, T., Montúfar, G., & Trager, M. (2022). Geometry of linear convolutional networks. *SIAM J. Appl. Algebra Geom.*, *6*(3), 368-406.

[4] Kohn, K., Montúfar, G., Shahverdi, V., & Trager, M. (2024). Function space and critical points of linear convolutional networks. *SIAM J. Appl. Algebra Geom.*, *8*(2), 333-362.

[5] Nguegnang, G.M., Rauhut, H., & Terstiege, U. (2021). Convergence of gradient descent for learning linear neural networks. Preprint, *arXiv:2108.02040*.

[6] Shahverdi, V. (2024). Algebraic complexity and neurovariety of linear convolutional networks. Preprint, *arXiv:2401.16613*.

[7] Trager, M., Kohn, K., & Bruna, J. (2020). Pure and spurious critical points: A geometric study of linear networks. In *8th international conference on learning representations*.

[8] Zhang, L., Naitzat, G., & Lim, L.-H. (2018). Tropical geometry of deep neural networks. In *Proceedings of the 35th international conference on machine learning (PMLR)* (pp. 5824-5832). Stockholm, Sweden.

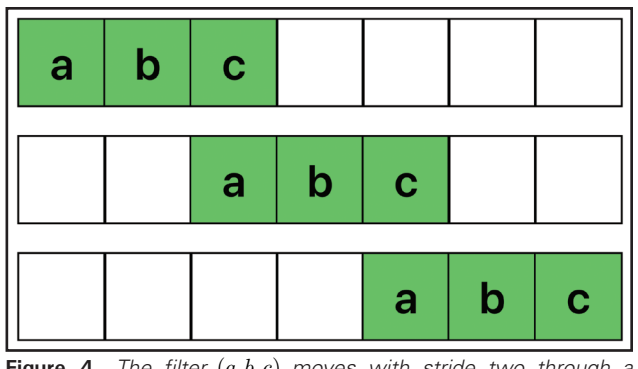

Figure 4. *The filter (a,b,c) moves with stride two through a vector of length seven and yields a linear convolution $\mathbb{R}^7 \to \mathbb{R}^3$, $(x_1,\dots,x_7) \mapsto (ax_1+bx_2+cx_3,\ ax_3+bx_4+cx_5,\ ax_5+bx_6+cx_7)$. Figure courtesy of the author.*

Kathlén Kohn is a tenure-track assistant professor at KTH Royal Institute of Technology in Sweden. Her research uses algebraic methods to investigate the underlying geometry in computer vision, machine learning, and statistical problems.

Artificial Intelligence

Continued from page 1

Here, $\mathcal{L}$ is a loss function (such as the square loss) and $\mathcal{R}$ is a regularization term.

(iii) Use the test data to analyze the trained neural network's ability to generalize to unseen data.

These steps lead to three particular research directions—expressivity, training, and generalization—that are associated with the three error components in a statistical learning problem: approximation error, error from the algorithm, and out-of-sample error.

The area of *expressivity* seeks to determine approximation properties of the considered class of neural networks with respect to certain "natural" function classes, while also typically accounting for the neural networks' required complexity in terms of the number of nonzero parameters (weights and biases). Expressivity is perhaps the most thoroughly explored mathematical research direction of AI. An early highlight was the development of the famous universal approximation theorem in the 1980s [6]. This theorem shows that we can approximate any continuous function up to an arbitrary degree for non-polynomial activation functions of shallow neural networks, which were state of the art at the time. Intriguingly, recent results prove that neural networks can simulate most known approximation schemes, including approximation by affine systems like wavelets and shearlets [4].

The difficulty of *training* stems from the optimization problem's high nonconvexity and the presence of spurious local minima, saddle points, and local maxima in the loss landscape. It is therefore particularly surprising that stochastic gradient descent seems to find "good" local minima in the resulting generalization performance. Achieving this success requires analysis of the loss landscape via a combination of training dynamics and techniques from areas such as algebraic geometry. One recent highlight is the phenomenon of *neural collapse* [11], wherein the class features form well-separated clusters in feature space during the final stages of training. This result helped us understand why training beyond the point of zero training error does not yield a highly overfitted model, as we might expect.

We can essentially subdivide *generalization* into two classes: functional analytic approaches and stochastic/statistical approaches. The first class typically aims for error bounds in deterministic settings. For example, we can precisely determine the generalization error of spectral graph convolutional neural networks for input graphs that model the same phenomenon, e.g., in the sense of graphons [9]. In contrast, the second class typically seeks to analyze the so-called double descent curve, which exhibits the surprisingly positive effects of overparameterization (see Figure 1, on page 1). Such analysis usually relies on methods like the Vapnik-Chervonenkis dimension, Rademacher complexity, or neural tangent kernels [7].

A deep mathematical understanding of expressivity, training, and generalization will be crucial to ensure reliability. However, the aforementioned EU AI Act and other similar regulations question whether reliability is achievable without detailed information about the entire training process. These policies ask for a "right to explanation" for AI technologies. Such requests lead to the concept of *explainability*, which aims to clarify the way in which neural networks reach decisions by determining and highlighting the main features of the input data that contribute to a particular decision. This ability would be highly useful for both explaining decisions to customers and deriving additional insights from data in scientific applications. One goal is to develop explainability approaches that enable human users to communicate with a neural network in the same way that they might communicate with a human; the advent of large language models has brought this vision one step closer to reality. But from a mathematical standpoint, such an approach must also be reliable itself. Several potential mathematically grounded explainability methods are presently available, such as Shapley values from game theory [13] and rate-distortion explanations from information theory [8].

While users are currently applying deep neural networks and AI techniques to a wide variety of problems in science and industry, these methods do have significant limitations. This research direction is unfortunately not a major focus at the moment, but some results are still worth highlighting. For example, recent work demonstrated that the minimal number of training samples to guarantee a given uniform accuracy on any learning problem scales exponentially in both the depth and input dimension of the network architecture; this means that learning ReLU networks to high uniform accuracy is intractable [2]. In 2022, another study analyzed the problem of running AI-based algorithms on digital hardware (like graphical processing units) that is modeled as a Turing machine, whereas the problems themselves are typically of a continuum nature [5]. Unfortunately, this discrepancy makes various problems—including inverse problems—noncomputable and causes serious reliability issues. At the same time, other results indicate that Blum-Shub-Smale machines—which relate to innovative analog hardware, such as neuromorphic chips or quantum computing—could surmount this obstacle [3]. Such hardware will hopefully also overcome the acute concern of energy consumption by digital hardware (see Figure 2), which is a key item in the U.S. CHIPS and Science Act.[4]

To summarize, unreliability is one of the most serious impediments in the development of AI technology, and many areas of mathematics will help address this complication. Furthermore, the automatic verification of properties that are legally required for AI-based approaches is only attainable through a mathematization of terms like the "right to explanation." AI reliability is hence inextricably linked to mathematics, ultimately creating very exciting research opportunities for our community.

References

[1] Berner, J., Grohs, P., Kutyniok, G., & Petersen, P. (2022). The modern mathematics of deep learning. In P. Grohs & G. Kutyniok (Eds.), *Mathematical aspects of deep learning* (pp. 1-111). Cambridge, U.K.: Cambridge University Press.

[2] Berner, J., Grohs, P., & Voigtlaender, F. (2023). Learning ReLU networks to high uniform accuracy is intractable. In *The eleventh international conference on learning representations (ICLR 2023)*. Kigali, Rwanda.

[3] Boche, H., Fono, A., & Kutyniok, G. (2022). Inverse problems are solvable on real number signal processing hardware. Preprint, *arXiv:2204.02066*.

[4] Bölcskei, H., Grohs, P., Kutyniok, G., & Petersen, P. (2019). Optimal approximation with sparsely connected deep neural networks. *SIAM J. Math. Data Sci.*, *1*(1), 8-45.

[5] Colbrook, M.J., Antun, V., & Hansen, A.C. (2022). The difficulty of computing stable and accurate neural networks: On the barriers of deep learning and Smale's 18th problem. *Proc. Natl. Acad. Sci.*, *119*(12), e2107151119.

[6] Cybenko, G. (1989). Approximation by superpositions of a sigmoidal function. *Math. Control Signals Syst.*, *2*, 303-314.

[7] Jacot, A., Gabriel, F., & Hongler, C. (2018). Neural tangent kernel: Convergence and generalization in neural networks. In *NIPS'18: Proceedings of the 32nd international conference on neural information processing systems* (pp. 8580-8589). Montreal, Canada: Curran Associates, Inc.

[8] Kolek, S., Nguyen, D.A., Levie, R., Bruna, J., & Kutyniok, G. (2022). A rate-distortion framework for explaining black-box model decisions. In A. Holzinger, R. Goebel, R. Fong, T. Moon, K.-R. Müller, & W. Samek (Eds.), *xxAI - Beyond explainable AI* (pp. 91-115). *Lecture notes in computer science* (Vol. 13200). Cham, Switzerland: Springer.

[9] Levie, R., Huang, W., Bucci, L., Bronstein, M., & Kutyniok, G. (2021). Transferability of spectral graph convolutional neural networks. *J. Mach. Learn. Res.*, *22*(1), 12462-12520.

[10] McCulloch, W.S., & Pitts, W. (1943). A logical calculus of the ideas immanent in nervous activity. *Bull. Math. Biophys.*, *5*, 115-133.

[11] Papyan, V., Han, X.Y., & Donoho, D.L. (2020). Prevalence of neural collapse during the terminal phase of deep learning training. *Proc. Natl. Acad. Sci.*, *117*(40), 24652-24663.

[12] Semiconductor Research Corporation (2021). *Decadal plan for semiconductors: Full report*. Durham, NC: Semiconductor Research Corporation. Retrieved from https://www.src.org/about/decadal-plan.

[13] Štrumbelj, E., & Kononenko, I. (2010). An efficient explanation of individual classifications using game theory. *J. Mach. Learn. Res.*, *11*(1), 1-18.

Gitta Kutyniok is Bavarian AI Chair for Mathematical Foundations of Artificial Intelligence at the University of Munich (LMU Munich), as well as director of the Konrad Zuse School of Excellence in Reliable AI. Her research focuses on applied harmonic analysis, artificial intelligence, compressed sensing, data science, deep learning, imaging science, inverse problems, and numerical analysis of partial differential equations.

[4] https://democrats-science.house.gov/chipsandscienceact

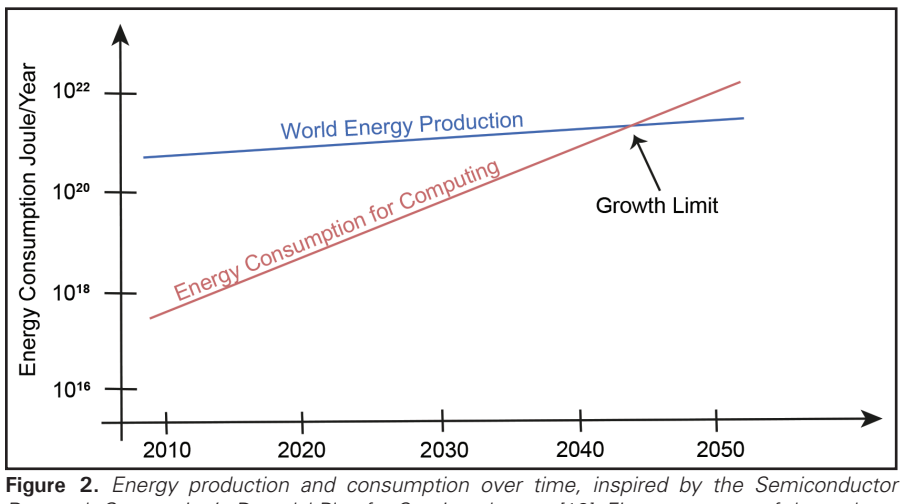

Figure 2. *Energy production and consumption over time, inspired by the Semiconductor Research Corporation's Decadal Plan for Semiconductors [12]. Figure courtesy of the author.*

The Importance of Mathematics in Political Decision-making

Mathematics in Politics and Governance. *By Francisco J. Aragón-Artacho and Miguel A. Goberna. Springer Nature, Cham, Switzerland, April 2024. 220 pages, $49.99.*

BOOK REVIEW
By Paul J. Nahin

Let me be perfectly clear (as politicians like to say, while often doing quite the opposite): *Mathematics in Politics and Governance* is not a perfect book. Several things about it—not many, but a few—concerned me. And yet … if I had to select just one mathematics book to take with me on a two-week sea cruise—on a ship with no library of mystery novels to distract me—and I wanted a text that would be challenging, informative, and intimately connected to the real world, this would be the one. Written by Spanish academic mathematicians Francisco Aragón-Artacho and Miguel Goberna, *Mathematics in Politics and Governance* offers numerous, quite specific examples (names are named!) of how the disparate worlds of hard-nosed, rigorous mathematical reasoning and soft, hand-wavy policymaking need not be mutually exclusive. To that end, the book is loaded with true-story politics, historical anecdotes, and lots of solid analyses that assume reader familiarity with college-level math.

The text opens with a story about U.S. President Abraham Lincoln. Lincoln admitted that he simply could not understand what it meant to *demonstrate* something during his early studies of the law; it wasn't until he mastered Euclid's geometry that he fully grasped the concept. The authors point out that most politicians typically remain in Lincoln's earlier, limited state of understanding and only possess a minimal knowledge of mathematics. Of course, there are rare exceptions. U.S. President James Garfield discovered an elegant new proof of the Pythagorean theorem while he was still a congressman, and former German Chancellor Angela Merkel holds a doctorate in quantum chemistry.

At the other end of the mathematical literacy spectrum, *Mathematics in Politics and Governance* offers numerous examples of politicians who fail to comprehend mathematics (or, depending on one's level of cynicism, seem to purposefully mislead). In one example, U.S. President Richard Nixon—whom Aragón-Artacho and Goberna call a "master illusionist"—asserted in a formal speech that "the pace of inflation change is slowing." As the authors observe, this claim is a subtle diversion from the actual price of goods to the *third derivative* of prices. Although Nixon was a Republican, the book has no particular axe to grind and we learn that Democratic U.S. President Barack Obama made similar mathematical missteps. Math illiteracy is a nonpartisan attribute.

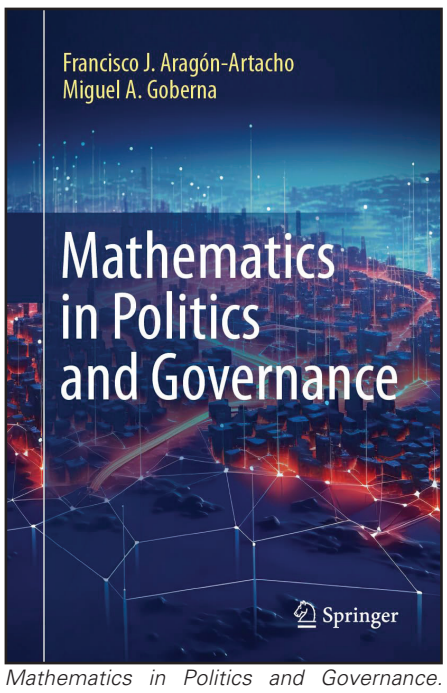

Mathematics in Politics and Governance. By Francisco Aragón-Artacho and Miguel Goberna. Courtesy of Springer Nature.

The application of math to societal problems likely began with the development of geometry; for instance, people presumably needed to re-establish property boundary lines after the annual flooding of the Nile. While that particular example is not in the book, the authors do present an interesting alternative illustration with the ancient Dido's problem: Given a city to be built on a river's straight shoreline, what curve of a fixed length (with its endpoints on the shoreline) includes the greatest area? The answer is of course a semicircle, and Aragón-Artacho and Goberna discuss Jakob Steiner's famous 1842 proof that uses only simple geometric arguments. They also demonstrate that town planners actually knew about this solution much earlier, as evidenced by a map of the German city of Cologne along the Rhine that is dated to 1800. The semicircle boundary is clearly visible.

From this point on, the book's math content becomes a bit more advanced. Commentary about various mathematical areas is embedded in specific examples of political scenarios that are generally presented as problems that optimize an objective function by some criteria. These scenarios span a broad swath of human concerns: healthcare, energy pricing, the allocation of scarce resources, and numerous other subjects where policy decisions are routinely made by politicians who may or may not understand the associated analytics. Linear programming and game theory in the context of nuclear war strategy lend themselves to particularly interesting dialogues. It may be asking too much for presidents to be familiar with such esoteric concepts, but we should all hope that several members of their support staff *are* math literate.

The appeal of *Mathematics in Politics and Governance* is greatly enhanced by numerous biographical sketches and photographs of the featured mathematicians. Also compelling is the authors' willingness to comment on some less-than-flattering episodes, such as the 1975 Nobel Economics Prize committee's outrageous snub of George Dantzig, despite his pioneering work on the simplex algorithm. Even the two men who shared the prize were stunned by the committee's disregard for Dantzig, and both mentioned their missing colleague in their acceptance speeches. Up to three individuals can receive the prize, so Dantzig's exclusion felt like a significant rebuff. It thus strikes me as somewhat ironic that Dantzig's photo is missing from the book. Also missing is *any* mention of Richard Bellman and dynamic programming. I realize that it is unfair to criticize a small book of only 200 or so pages for not including *everything*, but Bellman's omission seems like an oversight.

See **Political Decision-making** *on page 8*

Does Air Rotate with the Tire?

MATHEMATICAL CURIOSITIES
By Mark Levi

Does the air in a rolling tire rotate at the same speed as the tire, assuming that the tire has been rolling with constant speed for some time? This question is not quite as silly as it seems because the lower part of the tire is flattened by the road, which means that the air in the tire is continuously deformed.

Flow Induced by Squeezing

Imagine squeezing a tire in the vicinity of $\theta=\theta_0$, thus expelling the air particles away from θ_0 and moving them towards the diametrically opposite point $\theta_0+\pi$. The simplest imaginable expression for the resulting speed is

$$\dot\theta = a\sin(\theta-\theta_0), \qquad (1)$$

where θ stands for the angular coordinate of an air particle. We can think of the tire as a thin tube, like a bike tire. This is certainly not an accurate model, but it provides an excuse for some possibly amusing mathematical observations.

Flow in a Rolling Tire

In Figure 1, a rolling tire is simultaneously squeezed in the forward part of the flattened patch (segment OB) and released in the rear part (segment AO). According to (1), the resulting air motion is given by

$$\dot\theta = a\sin(\theta-\theta_0)-a\sin(\theta-\theta_1)=$$
$$2a\sin(\theta-\theta_m).$$

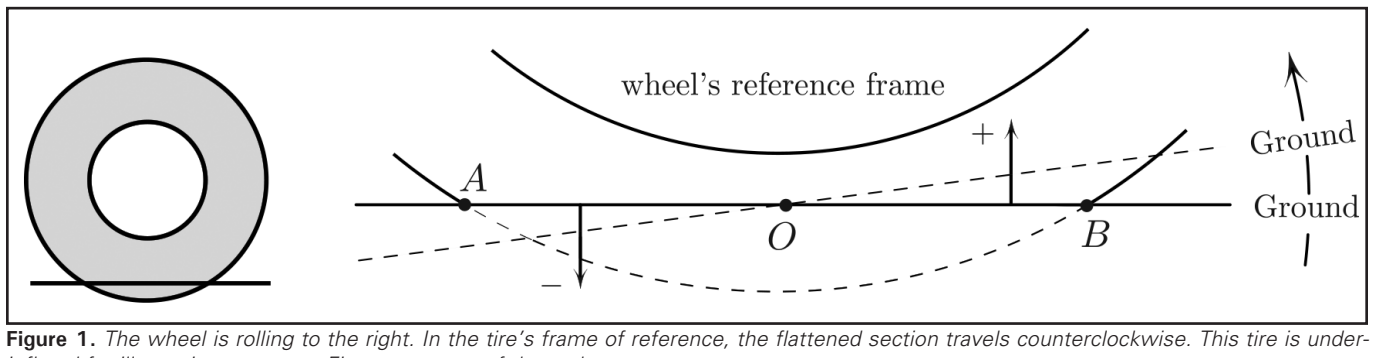

Figure 1. *The wheel is rolling to the right. In the tire's frame of reference, the flattened section travels counterclockwise. This tire is underinflated for illustrative purposes. Figure courtesy of the author.*

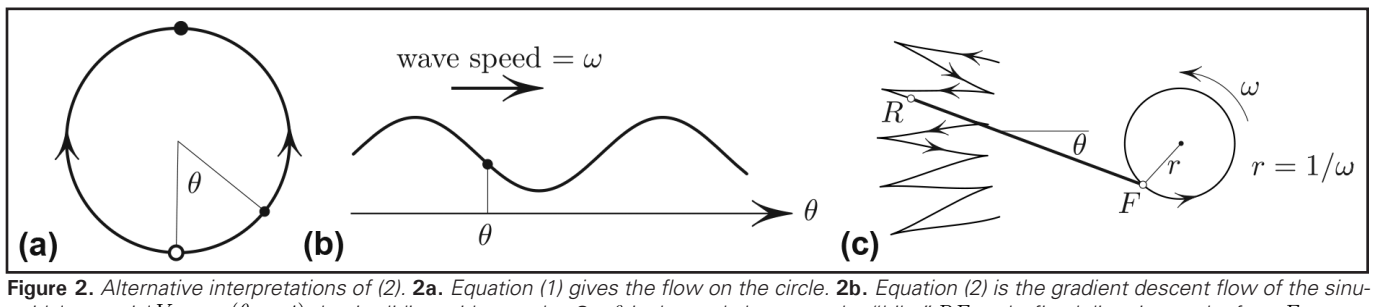

Figure 2. *Alternative interpretations of (2).* **2a.** *Equation (1) gives the flow on the circle.* **2b.** *Equation (2) is the gradient descent flow of the sinusoidal potential $V=\cos(\theta-\omega t)$ that is sliding with speed ω.* **2c.** *θ is the angle between the "bike" RF and a fixed direction as the front F moves in a circle of radius ω^{-1} with angular velocity ω. Each zigzag of R corresponds to one trip of F around the circle. Figure courtesy of the author.*

And since the tire is rolling, $\theta_m=\omega t$ (the ground rotates counterclockwise in the tire's frame, as in Figure 1). By taking $2a=1$ to minimize mess, we then have an angular velocity of air particles *in the wheel's reference frame*:

$$\dot\theta = \sin(\theta-\omega t). \qquad (2)$$

Figure 2 offers some alternative interpretations of (2):

1. θ moves down the gradient of the time-dependent potential $V(\theta,t)=\cos(\theta-\omega t)$. This movement is loosely akin to a cork bobbing on a wave that is traveling to the right with speed ω. Our initial question amounts to estimating the drift of the cork.

2. Consider a "bicycle," i.e., a moving segment RF of fixed length 1 in the plane. The velocity of the "rear" R is constrained to lie along RF so that R cannot "sideslip." Let us guide the "front" F around the circle of radius ω^{-1}, with angular velocity ω and unit speed F. The angle θ that is formed by RF with a fixed direction then satisfies (2).

A naive look at (2) may suggest zero drift, since the average of the right side with respect to both t and θ is zero. However, the "bike" interpretation in Figure 2 is a convincing indication that there *is* drift, i.e., that θ increases with a nonzero average speed.

Another convincing no-calculation argument for nonzero drift comes from looking at the limiting case of small ω (the opposite of the one in which we are interested). In this case, the wave in Figure 2 moves slowly and a typical solution is trapped by the potential's slowly moving well. The solution thus has the same drift ω as the wave, suggesting that the drift is positive for all ω — including $\omega\gg1$. For large ω, however, the drift speed is actually a decreasing function of ω (in contrast to the case of small ω).

Estimating the Drift for Large ω

The drift[1] for solutions of (2) for large ω turns out to be

$$\lim_{t\to\infty}\frac{\theta(t)}{t}=\frac{1}{2\omega}+O(\omega^{-2}). \qquad (3)$$

So, the air in our utterly idealized tire circulates backwards *relative to the tire* with angular velocity $\approx 1/2\,\omega$. For the ground observer, the air in the rolling tire rotates with the tire, but not quite as fast — namely, with the angular velocity $\omega-1/2\,\omega$. Equivalently, the "cork" on the wave in Figure 2b drifts slowly to the right with speed $1/2\,\omega$ when ω is large. The faster the wave, the slower the drift.

Proof of (3)

A routine proof of (3)—which I omit so as not to bore the reader—involves putting oneself into a moving frame by setting $\varphi=\theta-\omega t$ as the new dependent variable; doing so obtains an autonomous ordinary differential equation (ODE) that we can then solve in quadratures before expanding the result in powers of ω^{-1}. This method works for any ODE of the form $\dot\theta=v(\theta-\omega t)$—where v is a periodic function—and shows that the speed of the drift is

$$\frac{\overline{v^2}}{\omega}$$

See **Does Air Rotate** *on page 7*

[1] This is known as Stokes drift.

Modeling the Impact of Rainfall Variability on Vegetation in Drylands

By Lakshmi Chandrasekaran

The global population continues to face the detrimental effects of food insecurity and climate change, with an estimated 1.3 billion people having experienced food insecurity in 2022 [4]. At the 2023 United Nations Climate Change Conference[1] (COP28)—which took place last December in Dubai, the United Arab Emirates (UAE)—more than 150 countries endorsed the COP28 UAE Declaration on Sustainable Agriculture, Resilient Food Systems, and Climate Action.[2] This global commitment aims to better align countries' efforts to manage food systems and agriculture and adapt to the changing climate.

Given the urgency of this issue, existing mathematical models investigate the impact of changing rainfall levels on some of the driest regions on Earth. The Horn of Africa is a particularly well-studied location, as the distinct self-organized spatial patterns in this region are easily visible via satellite images. In fact, applied mathematician Mary Silber of the University of Chicago has employed mathematical models of terrain topography[3] to investigate the shape of vegetation patterns and their slow dynamics in drylands [1].

Previous modeling studies use mean annual rainfall levels as a bifurcation parameter to explore vegetation patterns on decadal (and longer) timescales. However, this approach does not resolve other features of rainfall, such as the intensity and timing of storms and their variability on short timescales. "These are fast processes—maybe hours—over short times, and we're simulating things on a year-long timescale," Punit Gandhi of Virginia Commonwealth University (a frequent collaborator of Silber) said.

To better associate mathematical models with the natural timescale of these processes, Silber, Gandhi, and Lily Liu (who was an undergraduate at the University of Chicago during this project and is currently a Ph.D. student at New York University) built upon an existing fast-slow switching model that contains fast hydrological processes and slow biomass dynamics [2]. The model's fast subsystem is represented with partial differential equations:

$$\frac{\partial H}{\partial T} = P(T) - I(H,W;B(X)) + \frac{\partial}{\partial X}(V(H;B(X))H), \quad (1)$$

$$\frac{\partial W}{\partial T} = I(H,W;B(X)), \quad (2)$$

where H is the surface water height, W is the soil water column height, and B is the biomass density. Here, $H(X,T)$ evolves on a short timescale of rain events, $B(X,T)$ evolves on a long timescale between rain events, and $W(X,T)$ corresponds to several processes that act on both fast and slow timescales. The first, second, and third terms on the right side of (1) respectively denote precipitation, soil infiltration, and advection. The infiltration rate I is modeled as a function of surface water height, soil water column height, and biomass density. The important positive feedbacks between biomass and soil moisture distribution come from I (which is higher when biomass is present) and the flow speed function V (which is slower when vegetation is present, allowing more time for infiltration).

Biomass and soil water evolve on a slow timescale that is associated with plant growth; they are governed by

$$\frac{\partial W}{\partial T} = -(L + \Gamma B)W + D_W \frac{\partial^2 W}{\partial X^2}, \quad (3)$$

$$\frac{\partial B}{\partial T} = C\left(1 - \frac{B}{K_B}\right)\Gamma B W - MB + D_B \frac{\partial^2 B}{\partial X^2}. \quad (4)$$

This subsystem evolves the soil water $W(X,T)$ and is initialized by the post-storm distribution $W(X)$ and biomass density $B(X,T)$. The two terms on the right side of (3) denote evapotranspiration and diffusion, the parameter L represents the evaporation rate, and ΓB signifies the transpiration rate. In (4), the three right terms respectively denote growth, death, and dispersal. The death rate M is constant and the dispersal is modeled via linear diffusion. Transpiration dictates the biomass growth rate, whose efficiency is set by C.

In a recent paper that published in the *SIAM Journal of Applied Dynamical Systems*[4] last year, Gandhi, Liu, and Silber expanded this existing framework to create a mathematical model that explores rainfall pattern variability over shorter timescales and its corresponding impact on the formation of vegetation patterns in dry ecosystems [3]. The climatology of the Horn of Africa inspired this new *pulsed-precipitation model*, which represents rainstorms as instantaneous "kicks" to the soil water—i.e., Dirac delta function impulses that deposit a uniform layer of water on the surface.

Though they retained the same reaction-diffusion model in the slow subsystem, the team made two significant changes to the fast subsystem that allowed them to determine the output soil moisture distribution $W(X)$ in a closed-form expression. First, the term $P(T)$ in (1) now signifies rain events that instantaneously deposit a uniform water column of height H_0. The timing and strength of these precipitation pulses are the random variables in the stochastic simulations. And second, the infiltration rate I is now given by

$$I(H,B(X)) \equiv K_I\left(\frac{B(X)+fQ}{B(X)+Q}\right)\Theta(H). \quad (5)$$

The Heaviside unit step function $\Theta(H)$ indicates that the infiltration is independent of soil saturation and is modeled as a simple on-off switch in the presence or absence of surface water, assuming that $\Theta(0) = 0$.

Using these modifications, the researchers reformulated the fast-slow model to a pulsed-precipitation framework in which the rainstorm instantaneously deposits water on the surface at a fast timescale, after which an intervening dry period evolves on a slow timescale. This new model reveals interesting insights about rainfall patterns. Figure 1a illustrates the time series for periodic rainfall during the last two years of a 100-year simulation. Figure 1b depicts spatial profiles—derived from the simulation's final year—that compare soil water and biomass given the farthest distance that surface water travels before infiltration during a rainstorm. Figure 1c then offers a time series of total annual rainfall, along with the five-band spacing of annually averaged soil water and biomass. Similarly, Figure 2 presents the simulated results for stochastic rainfall in the form of a stochastic traveling wave solution that fluctuates based on season and rainfall variability.

Figure 3 compares patterns under periodic and stochastic rainfall in a smaller domain than Figures 1 and 2. The team changed the size of the periodic domain L to enforce different band spacings and restricted L to less than 250 meters (m). When L ranges from 100-167 m or falls under 59 m, the simulations do not exhibit a traveling wave state with periodic rainfall. But for these values of L in the case of stochastic rainfall, the simulations do show a stochastic traveling wave. "It was surprising to find that under periodic rainfall, we sometimes saw crazy behavior," Gandhi said.

Gandhi and his collaborators utilized linear stability analysis techniques to explain these differences. Using the periodic rainfall scenario with uniform vegetation in the pulsed-precipitation model, they introduced a small sinusoidal perturbation to the initial state to see whether it would grow into a full vegetation band. The researchers found that for mean annual precipitation (MAP) values that were greater than roughly 43 centimeters, the perturbation dampens and yields uniform vegetation (see Figure 4, on page 7). But as the MAP decreases to lower values (which is expected in arid regions like the Horn of Africa), the analysis—in the presence of spatially periodic perturbation—reveals resonance tongues across multiple regions with growing vegetation patterns.

This finding proves that the regularity of "artificial" periodic rainfall patterns

See **Vegetation in Drylands** *on page 7*

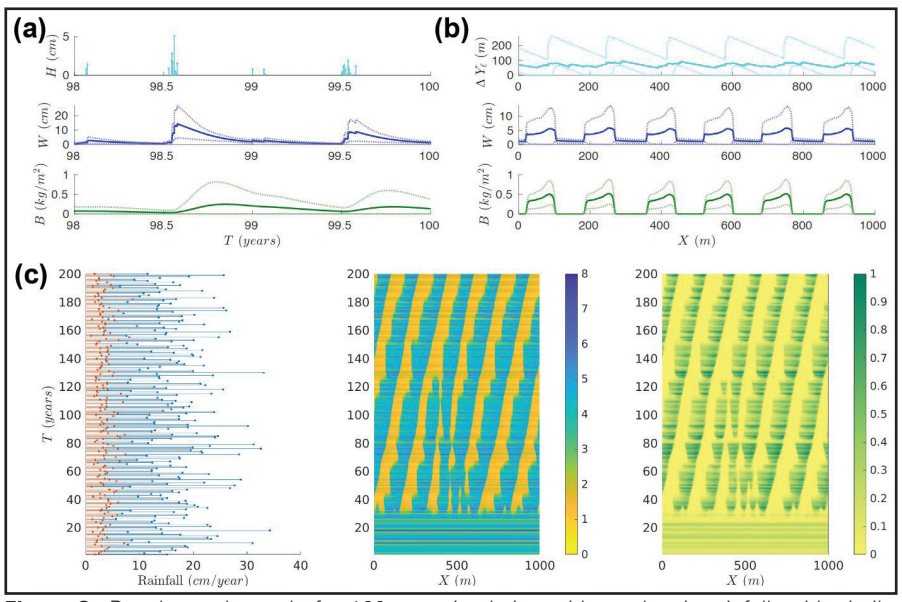

Figure 2. *Results at the end of a 100-year simulation with stochastic rainfall, with similar parameters to Figure 1.* **2a.** *Time series during the last two years of the simulation.* **2b.** *Spatial profiles of surface water travel distance, soil water, and biomass that are derived from the simulation's final year.* **2c.** *Time series of annual rainfall and spacetime plots of annually averaged soil water and biomass. Figure courtesy of [3].*

[1] https://unfccc.int/cop28

[2] https://www.cop28.com/en/food-and-agriculture

[3] https://sinews.siam.org/Details-Page/modeling-vegetation-patterns-in-vulnerable-ecosystems

[4] https://www.siam.org/publications/journals/siam-journal-on-applied-dynamical-systems-siads

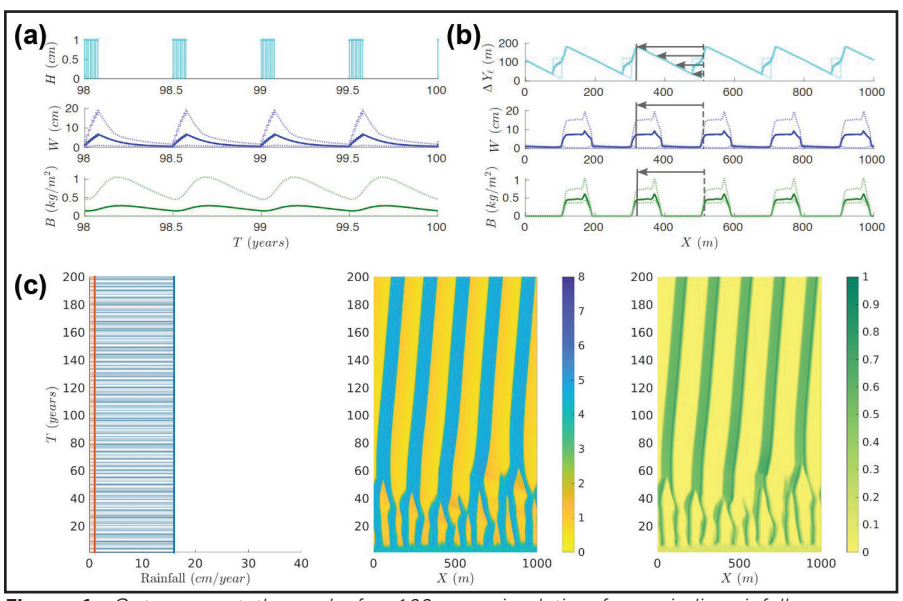

Figure 1. *Outcomes at the end of a 100-year simulation for periodic rainfall on a one-kilometer domain that is sloped uphill towards the right. The mean annual precipitation is 16 centimeters (cm) and the mean storm depth is $H_0 = 1$ cm.* **1a.** *Time series during the last two years of the simulation.* **1b.** *Spatial profiles that are derived from the simulation's final year. The vertical axis of the top panel refers to the farthest distance that surface water travels during a rainstorm before it infiltrates the ground at point X. The lower two panels are profiles for soil water and biomass.* **1c.** *The left panel is a time series of total annual rainfall (in blue), with a 1 cm contribution from each rainstorm (in orange). The middle and right panels respectively portray the five-band spacing of annually averaged soil water and biomass. The heat maps indicate less to more water or biomass, with colors ranging from yellow (at 0) to dark blue (at 8) or dark green (at 1). Figure courtesy of [3].*

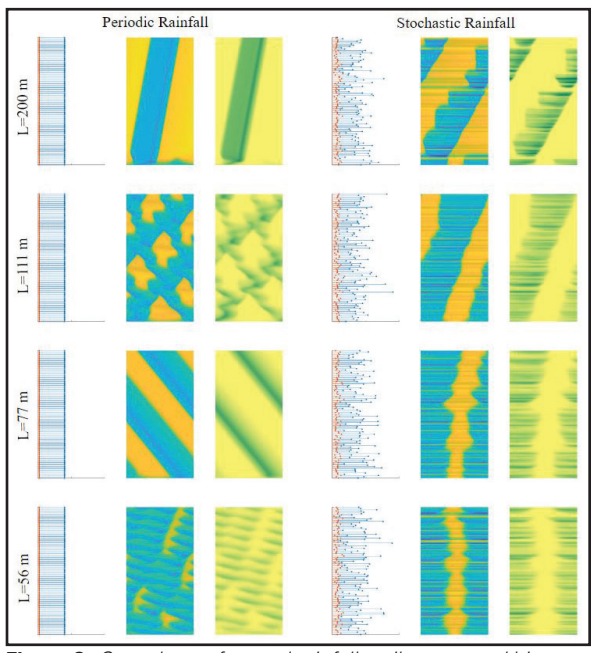

Figure 3. *Snapshots of annual rainfall, soil water, and biomass at different domain sizes L for periodic and stochastic rainfall. In each scenario, the vertical axis spans 100 years and the horizontal rainfall axis spans 40 centimeters (cm). The model parameters are fixed at a mean annual precipitation of 16 cm and a mean storm depth of $H_0 = 1$ cm. Figure courtesy of [3].*

Vegetation in Drylands

Continued from page 6

could lead to spatial resonance that in turn controls the preferred spacing of the vegetation bands. Specifically, vegetation band spacing is determined by the distance that surface water travels in the time that it takes for the precipitation pulse to fully infiltrate the soil. "The important thing to note is that the surface hydrology, which happens on timescales of seconds or minutes during storms, controls this large-scale vegetation pattern that evolves over decades," Gandhi said. Further simulations revealed that even during stochastic rainfall, the distance that water travels on the surface is a key component of pattern formation.

The pulsed-precipitation model reveals many interesting MAP insights, but a major question prevails: How will climate change influence these patterns? To investigate, the collaborators explored the implications of storm depth and rainy season duration on vegetation patterns. They found that longer rainy seasons—which correspond to shorter dry intervals, during which the biomass can survive without rain—could increase the vegetation's mean survival time. Similarly, more frequent but less intense storms—which are associated with a reduction in seasonal rainfall variability—could help prevent vegetation collapse.

The disappearance of spatial resonance with stochasticity in the rainfall model presents an intriguing mathematical challenge that merits further exploration. Many math modelers study vegetation patterns in vulnerable ecosystems under a changing climate, but Silber notes that this focus alone is not enough. "We also need to be thinking about water because it's a tightly coupled system," she said. "You have to think about the resource and the time in which water is acting."

While previous vegetation models have drawn tremendous inspiration from historical papers, Gandhi, Silber, and Liu's efforts highlight the vast potential for interdisciplinary collaborations. For instance, their current work could spur investigations into a variety of research problems, such as the use of mathematical models to inform measurable quantities for remote sensing of moisture, or model validation via feedback from field-based hydrology monitoring efforts. Most importantly, however, this study highlights the intricate interplay between the timescales of fast-acting hydrological processes and slowly evolving dryland vegetation patterns. A thorough understanding of these interactions may help future researchers assess the resilience of dryland ecosystems.

References

[1] Chandrasekaran, L. (2017). Modeling vegetation patterns in vulnerable ecosystems. *SIAM News*, *50*(2), 6.

[2] Gandhi, P., Bonetti, S., Iams, S., Porporato, A., & Silber, M. (2020). A fast-slow model of banded vegetation pattern formation in drylands. *Phys. D: Nonlinear Phenom.*, *410*, 132534.

[3] Gandhi, P., Liu, L., & Silber, M. (2023). A pulsed-precipitation model of dryland vegetation pattern formation. *SIAM J. Appl. Dyn. Sys.*, *22*(2), 657-693.

[4] Zereyesus, Y.A., & Cardell, L. (2022, November 8). Global food insecurity grows in 2022 amid backdrop of higher prices, Black Sea conflict. *U.S. Department of Agriculture: Amber Waves*. Retrieved from https://www.ers.usda.gov/amber-waves/2022/november/global-food-insecurity-grows-in-2022-amid-backdrop-of-higher-prices-black-sea-conflict.

Lakshmi Chandrasekaran holds a Ph.D. in mathematical sciences from the New Jersey Institute of Technology and a master's degree in science journalism from Northwestern University. She is a freelance science writer whose work has appeared in MIT Technology Review, Quanta, Science News, and other outlets.

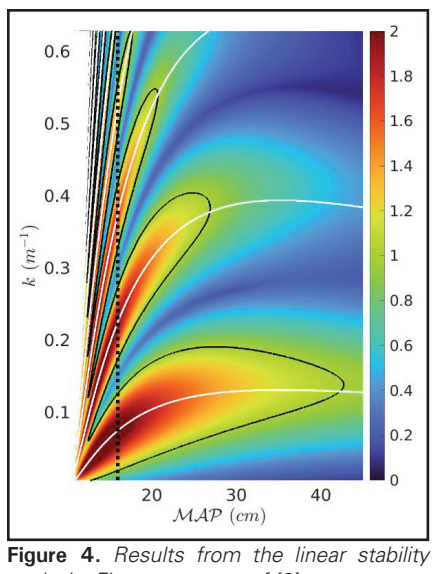

Figure 4. *Results from the linear stability analysis. Figure courtesy of [3].*

Does Air Rotate

Continued from page 5

to the leading order.[2] This expression indeed agrees with (3) for $v = \sin$.

Here, instead, is a shortcut to (3) that uses the following fact about "bicycles," i.e., unit length segments RF where the velocity of R is constrained to the direction RF: *Let the front F trace a closed path of small diameter δ enclosing area A and returning to the starting point. The segment RF then rotates around F through the angle*

$$\Delta\theta = A + o(\delta^2). \tag{4}$$

The Prytz planimeter (also called the hatchet planimeter)—a simple device that measures areas—is based on this observation. Details about this interesting topic are available in [1].

Now, (4) yields (3) almost immediately. Indeed, one revolution of F around the circle in Figure 2 (on page 5) results in $\Delta\theta = \pi r^2 + o(r^2)$, where $r = 1/\omega$. And the time of one revolution of F is $\Delta t = 2\pi/\omega$, since $\omega \stackrel{def}{=} 2\pi/\Delta t$. The speed of the drift is thus

$$\frac{\Delta\theta}{\Delta t} = \frac{\pi r^2 + o(r^2)}{2\pi/\omega} \stackrel{r=1/\omega}{=} \frac{1}{2\omega} + o(\omega^{-1}),$$

which confirms (3).

I would like to conclude with two puzzles for possible amusement.

Puzzles

Puzzle 1: The speed of the drift is an increasing function of ω for small ω and a decreasing function for large ω. Which ω maximizes the drift speed?

Puzzle 2: On another note, the subject of bikes came up twice already in this article: first in the initial question and second (in a completely different way) in Figure 2 (on page 5). This gives an excuse for another bike tire question that came to mind after I saw a bike at the bottom of the Limmat river in Zurich, Switzerland. Some miscreant probably threw the bike in, and I must reluctantly acknowledge that anonymous vandal's contribution; without him, this puzzle would not have arisen.

Assume that the air pressure in the bike tire was initially 2 atmospheres before it was thrown from the bridge and sunk to the depth of 10 meters.[3] Now the tire is squeezed from the outside by an additional pressure of 1 atmosphere. With this added compression, is the new pressure inside the tire $2 + 1 = 3$ atmospheres?

References

[1] Foote, R., Levi, M., & Tabachnikov, S. (2013). Tractrices, bicycle tire tracks, hatchet planimeters, and a 100-year-old conjecture. *Am. Math. Mon., 120*(3), 199-216.

Mark Levi (levi@math.psu.edu) is a professor of mathematics at the Pennsylvania State University.

[2] Here, $\overline{f}$ denotes the average of a function f.

[3] I chose a round number for the depth, but the river was of course less deep.

LS24 Panel Overviews Industry and Government Career Prospects in the Life Sciences

By Lina Sorg

The evolving nature of research and development in industry and government presents many exciting opportunities for applied and computational mathematicians who work in the life sciences. This broad subject area addresses a multitude of problems at various spatial, temporal, and organizational scales, with applications that range from biology, medicine, and epidemiology to climate change and even social justice. During the 2024 SIAM Conference on the Life Sciences[1] (LS24)—which took place this June in Portland, Ore.—a panel[2] of five researchers from industry and national laboratories reflected on their personal career trajectories, commented on the necessary background knowledge and skill-sets for life science projects, and offered advice to junior scientists who are seeking employment. The session was moderated by Nessy Tania of Pfizer and included panelists Sara Del Valle of Los Alamos National Laboratory (LANL), Elamin Elbasha of Merck & Co., Khamir Mehta of Amgen, Paul Patrone of the National Institute of Standards and Technology (NIST), and Monica Susilo of Genentech.

Although all five panelists currently enjoy successful careers in the life sciences, this particular field was not necessarily part of their original plans. As an undergraduate student, Patrone studied philosophy at St. John's College, a small liberal arts institution in Annapolis, Md. After reading many philosophical publications *about* math and science, he realized that he wanted to contribute directly to the discipline. While pursuing his Ph.D. in physics at the University of Maryland, College Park, Patrone began working at NIST; apart from a brief stint at Boeing after graduation, he has remained there ever since. "We have a very high-level view not only on science itself, but on mathematics," he said of his role as a staff scientist within NIST's Applied and Computational Mathematics Division. "We have some of the best experimentalists in the world."

Elbasha's professional journey also began in a completely different area of study. After obtaining undergraduate and M.A. degrees in economics in Sudan and Egypt respectively, he received a scholarship to the University of Minnesota and eventually earned a Ph.D. in agricultural and applied economics. Although Elbasha initially intended to become a professor, difficulties in securing an academic role led him to accept a position as an economist at the Centers for Disease Control and Prevention: his first foray into public health.

Now with more than 25 years of experience in the pharmaceutical sector, Elbasha is the executive director of Health Economic Decision Sciences at Merck, where he leads a group of quantitative scientists and applied mathematicians who create mathematical models of infectious diseases and assess the value of vaccines. "I know I can make a difference," he said. "It's rewarding to know that you're improving someone's life and making it safer."

Susilo shares the same sentiment about her position as a modeling and simulation scientist in the field of clinical pharmacology, which supports clinical trials and identifies doses/regimens that are both safe and efficacious. At Genentech, she routinely collaborates with clinicians and safety scientists on all aspects of drug development. "I love that I'm applying what I know from simulations and working with everyone on one goal: to get the best dose for the patient," Susilo said.

CAREERS IN MATHEMATICAL SCIENCES

Susilo's introduction to clinical pharmacology marked a significant shift from her previous studies. Prior to a postdoctoral appointment at Pfizer, she was completely unfamiliar with mathematical pharmacology — having completed her Ph.D. research on the mechanics of soft tissue. Luckily, she found that much of her mechanical engineering education was transmissible to a pharmacological career.

Mehta, who holds a degree in chemical engineering, concurred with Susilo about the transferability of the engineering toolkit. When he was a junior researcher and began to think seriously about his future, he decided that he wanted to make a positive change to existing protocols. Now, Mehta utilizes systems models to explore drug development processes at Amgen. "Seeing whether we can make more sense of a system by using more complex mathematics has been driving my work thus far," he said.

As a senior scientist at LANL, Del Valle leads an interdisciplinary team that investigates infectious diseases from the level of differential equations to large, agent-based simulations. These studies fall under the umbrella of national security, which is LANL's area of focus. Del Valle initially accepted an internship at LANL as a Ph.D. student at the University of Iowa and has been there ever since. "I never really thought that I would end up working at a national lab," she said. "I assumed I would teach mathematics because I thought that's what most mathematicians did."

Del Valle spoke highly of the national laboratories' interdisciplinary nature, which sets them apart from traditional academic institutions. She explained that mathematicians, physicists, computer scientists, and biologists frequently collaborate to generate solutions for complicated problems. "Most of the teams we have are very interdisciplinary," Del Valle said of LANL. "A diverse set of ideas, diverse people, and diverse approaches bring about breakthroughs, and that's one of the things I like about Los Alamos."

Because most jobs in industry or government involve at least some sort of multidisciplinary collaboration, the panelists all agreed that scientific and technical communication skills are paramount. "Around 80 percent of my work is writing proposals and papers and communicating with decision-makers and sponsors," Del Valle said. "Being able to communicate complex terms and sophisticated models to a decision-maker or sponsor who does not have any scientific background is key."

Elbasha agreed, noting that quantitative scientists often do not utilize the same frameworks as their colleagues from other disciplines — even though everyone is working towards a common objective. "You'll be dealing with really smart people, but the language is different," he said. "Learning how to work within a multidisciplinary team is one of the best skills you can have in an industrial environment."

Patrone is thankful for his liberal arts education, which trained him to communicate effectively and ask pertinent questions to better understand a problem: fundamental skills that are remarkably valuable during the interview process. As such, he is especially impressed by candidates who ask insightful questions, demonstrate an interest in both the company and its projects, and can think on their feet. "I want to see if you have an idea about how to tackle a problem," Patrone said. "The most interesting questions are the ones that people don't have an answer to. And if someone shows the initiative, that's a good person to hire."

When an audience member inquired about the role of machine learning (ML) in the current landscape, Del Valle confirmed that LANL utilizes the technology in nearly all of its projects to better interpret the data at hand. While Patrone affirmed the power of ML, he cautioned attendees to remain cognizant of the associated uncertainty penalties. "Having machine learning in your toolbox is useful, but it's just as important to try to understand it as a fundamental tool and recognize its limits as well as its strengths," he said. In addition to ML, the panelists concurred that coursework in linear algebra, differential equations, computer programming, and statistics is equally useful for industrial careers.

Next, conversation turned to top strategies for finding and applying to internships and job openings. As a general rule, Susilo encouraged attendees to seek out internship listings on company websites and career portals early in the calendar year, especially between January and March. Patrone added that NIST advertises many positions—including the National Research Council postdoctoral program[3]—on its website[4] and collaborates with neighboring universities in the Washington, D.C., area to find suitable candidates. Merck,[5] Amgen,[6] Genentech,[7] and LANL[8] similarly publicize permanent openings, postdoctoral opportunities, and summer programs online. But while online sources—including platforms such as LinkedIn—are typically the best places to find individual job listings, it is beneficial to have an internal contact when it comes to actually submitting an application; otherwise, one's file might get lost in the shuffle.

If job seekers do not personally know someone at a company of interest, Del Valle encouraged them to reach out to employees with whom they would like to work prior to submitting their materials. "We get 1,000 applications a day, maybe more," she said of LANL. "It's very overwhelming to look through all of those applications." However, Del Valle acknowledged that she cannot respond to all of the inquiries that she receives due to their sheer volume; as such, she is more likely to reply if a message comes from a trusted contact or personal acquaintance on behalf of a prospective applicant.

SIAM plays a critical role in helping junior scientists make valuable connections that grow their networks, set them up for long-term success, and increase their desirability in the job market. Mehta urged audience members to attend SIAM Career Fairs,[9] which allow students and early-career researchers to forge direct connections with actively recruiting companies. Elbasha noted that Merck has hired employees via postings on SIAM's Career Center,[10] as well as through similar pages of other mathematical and scientific societies. And of course, conferences like LS24 serve as prime occasions for early-career attendees to get acquainted with more senior colleagues.

When crafting application documents, individuals should personalize their cover letters as much as possible, avoid generics, and demonstrate their skills' relevancy to the job requirements. Candidates should also show that they are excited about the position and understand its responsibilities and logistics. Finally, Patrone reminded listeners that enthusiasm goes a long way — especially because most positions offer some amount of on-the-job training. "Nothing beats hunger," he said. "I've seen people come from behind because they really wanted something. People can have skills, but if you don't have hunger then you won't succeed."

Lina Sorg is the managing editor of SIAM News.

[1] https://www.siam.org/conferences/cm/conference/ls24

[2] https://meetings.siam.org/sess/dsp_programsess.cfm?SESSIONCODE=80678

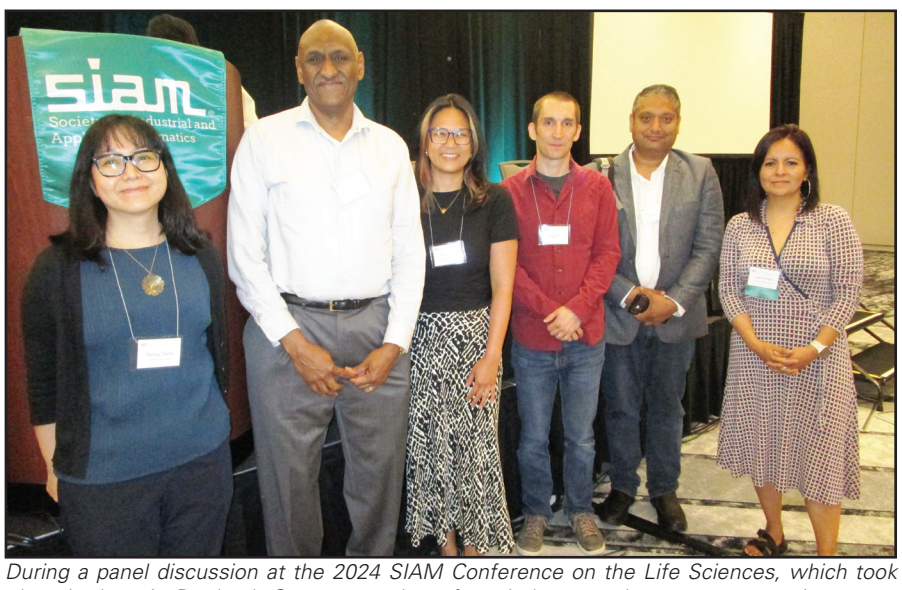

During a panel discussion at the 2024 SIAM Conference on the Life Sciences, which took place in June in Portland, Ore., researchers from industry and government settings commented on their respective experiences with mathematical careers in the life sciences and fielded questions from the audience. From left to right: moderator Nessy Tania of Pfizer and panelists Elamin Elbasha of Merck & Co., Monica Susilo of Genentech, Paul Patrone of the National Institute of Standards and Technology, Khamir Mehta of Amgen, and Sara Del Valle of Los Alamos National Laboratory. SIAM photo.

[3] https://www.nist.gov/iaao/academic-affairs-office/postdoctoral-students-nrc-postdocs

[4] https://www.nist.gov/itl/math/how-work-us

[5] https://jobs.merck.com/us/en

[6] https://careers.amgen.com/en/search-jobs

[7] https://careers.gene.com/us/en

[8] https://lanl.jobs

[9] https://www.siam.org/careers/resources/siam-career-fairs

[10] https://jobs.siam.org

Political Decision-making

Continued from page 5

Finally, one glaring problem—which is particularly irritating because it would have been so easy to avoid—is the complete absence of proper names in an already anemic index. During the copyediting phase, Springer provides software support that *automatically* generates an index *if* authors simply submit a list of entries. Why Aragón-Artacho and Goberna did not include proper names is a mystery to me.

Yet despite these minor grumblings, *Mathematics in Politics and Governance* is well worth a read. Just take my advice and pencil proper names into the index — the next time you read it and want to look up Dantzig or anybody else, you'll be very glad that you did!

Paul J. Nahin is a professor emeritus of electrical engineering at the University of New Hampshire. He is the author of 25 books on mathematics, physics, and electrical engineering; his latest book, How to Compute It When You Can't Solve It, will be published by Princeton University Press in late 2025.

InsideSIAM

Conferences, books, journals, and activities of Society for Industrial and Applied Mathematics

siam | CONFERENCES

A Place to Network and Exchange Ideas

Upcoming Deadlines

SIAM Conference on Mathematics of Data Science (MDS24)

October 21–25, 2024 | Atlanta, Georgia, U.S.
go.siam.org/mds24 | #SIAMMDS24

ORGANIZING COMMITTEE CO-CHAIRS
Eric Chi, *Rice University, U.S.*
David Gleich, *Purdue University, U.S.*
Rachel Ward, *University of Texas at Austin, U.S.*

EARLY REGISTRATION RATE DEADLINE
September 18, 2024

HOTEL RESERVATION DEADLINE
September 18, 2024

ACM-SIAM Symposium on Discrete Algorithms (SODA25)

January 12–15, 2025 | New Orleans, Louisiana, U.S.
go.siam.org/soda25 | #SIAMDA25

PROGRAM COMMITTEE CO-CHAIRS
Yossi Azar, *Tel-Aviv University, Israel*
Debmalya Panigrahi, *Duke University, U.S.*

EARLY REGISTRATION RATE DEADLINE
December 9, 2024

HOTEL RESERVATION DEADLINE
December 9, 2024

SIAM Symposium on Algorithm Engineering and Experiments (ALENEX25)

January 12–13, 2025 | New Orleans, Louisiana, U.S.
go.siam.org/alenex25 | #ALENEX25

PROGRAM COMMITTEE CO-CHAIRS
Jonathan Berry, *Sandia National Laboratories, U.S.*
Kathrin Hanauer, *University of Vienna, Austria*

SUBMISSION DEADLINE
July 18, 2024

SIAM Symposium on Simplicity in Algorithms (SOSA25)

January 13–14, 2025 | New Orleans, Louisiana, U.S.
go.siam.org/sosa25 | #SOSA25

PROGRAM COMMITTEE CO-CHAIRS
Ioana Bercea, *KTH Royal Institute of Technology, Sweden*
Rasmus Pagh, *University of Copenhagen, Denmark*

SUBMISSION DEADLINES
August 5, 2024: Short Abstract Submission and Paper Registration
August 8, 2024: Full Paper Submission

SIAM Conference on Computational Science and Engineering (CSE25)

March 3–7, 2025 | Fort Worth, Texas, U.S.
go.siam.org/cse25 | #SIAMCSE25

ORGANIZING COMMITTEE CO-CHAIRS
David Bindel, *Cornell University, U.S.*
Elizabeth Cherry, *Georgia Institute of Technology, U.S.*
Judith Hill, *Lawrence Livermore National Laboratory, U.S.*

SUBMISSION DEADLINES
August 5, 2024: Minisymposium Proposal Submissions
September 3, 2024: Contributed Lecture, Poster, Miniposterium and Minisymposium Presentation Abstracts

Information is current as of June 26, 2024. Visit *siam.org/conferences* for the most up-to-date information.

Students and Early Career Researchers: Apply Now for Conference Support

SIAM is dedicated to giving students and early career professionals the support they need to be successful. The SIAM Travel Awards Program awards $240,000+ in conference travel funding yearly to these two groups. Apply now at *siam.smapply.org/prog/travel_awards_program*.

Upcoming SIAM Events

2024 SIAM Annual Meeting
July 8–12, 2024
Online Component July 18–20, 2024
Spokane, Washington, U.S.

SIAM Conference on Applied Mathematics Education
July 8–9, 2024
Spokane, Washington, U.S.
Sponsored by the SIAM Activity Group on Applied Mathematics Education

SIAM Conference on Discrete Mathematics
July 8–11, 2024
Spokane, Washington, U.S.
Sponsored by the SIAM Activity Group on Discrete Mathematics

ICERM-SIAM Workshop on Empowering a Diverse Computational Mathematics Research Community
July 22–August 2, 2024
Providence, Rhode Island, U.S.

SIAM Activity Group on Equity, Diversity, and Inclusion Business Meeting
July 29, 2024 at 12:00 p.m. / Online
Sponsored by the SIAM Activity Group on Equity, Diversity, and Inclusion

GLSIAM Meeting 2024
October 12, 2024
Hammond, Indiana, U.S.

SIAM Conference on Mathematics of Data Science
October 21–25, 2024
Atlanta, Georgia, U.S.
Sponsored by the SIAM Activity Group on Data Science

Bulgarian Section of SIAM Annual Meeting 2024
December 9–11, 2024
Sofia, Bulgaria

ACM-SIAM Symposium on Discrete Algorithms
January 12–15, 2025
New Orleans, Louisiana, U.S.
Sponsored by the SIAM Activity Group on Discrete Mathematics and the ACM Special Interest Group on Algorithms and Computation Theory

SIAM Symposium on Algorithm Engineering and Experiments
January 12–13, 2025
New Orleans, Louisiana, U.S.

SIAM Symposium on Simplicity in Algorithms
January 13–14, 2025
New Orleans, Louisiana, U.S.

SIAM Conference on Computational Science and Engineering
March 3–7, 2025
Fort Worth, Texas, U.S.
Sponsored by the SIAM Activity Group on Computational Science and Engineering

SIAM International Conference on Data Mining
May 1–3, 2025
Alexandria, Virginia, U.S.
Sponsored by the SIAM Activity Group on Data Science

siam | MEMBERSHIP

Network | Access | Outreach | Lead

Annual SIAM Membership Report

As of December 31, 2023, SIAM had 12,791 members from 103 countries. Forty percent (40%) of SIAM members reside outside the United States. The charts on this page show information about SIAM members.

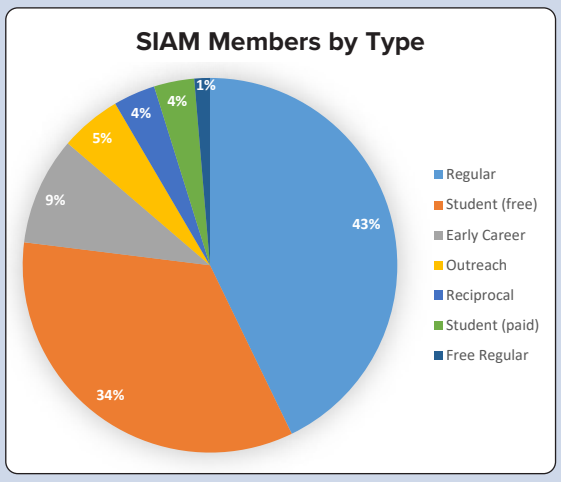

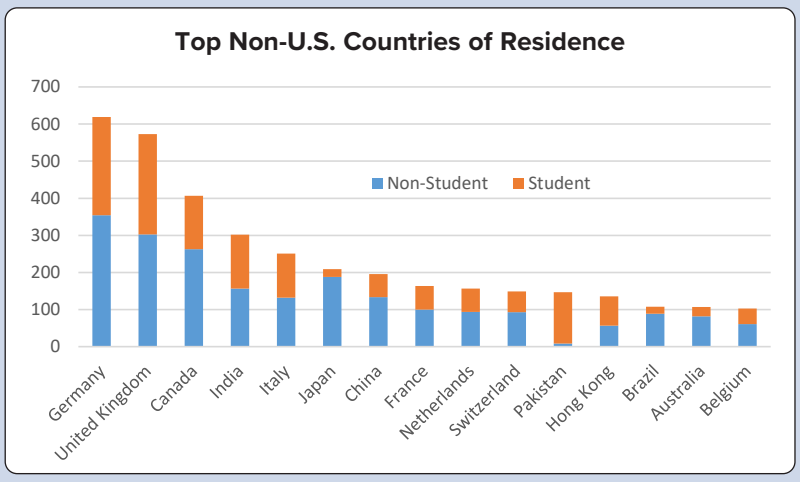

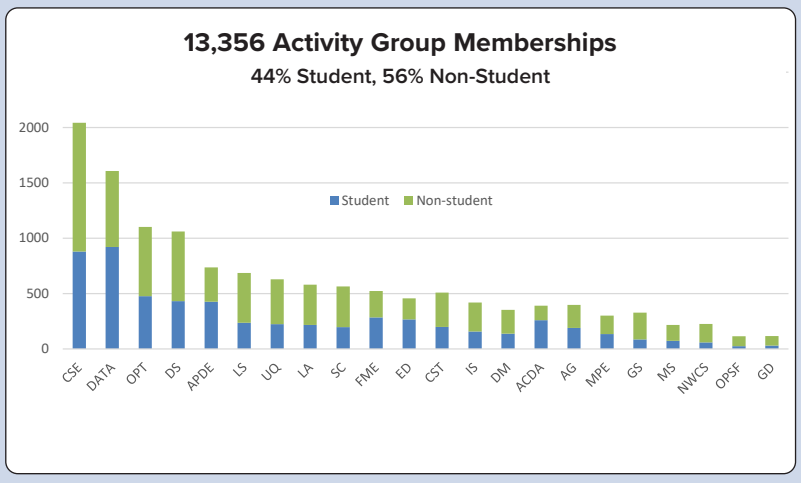

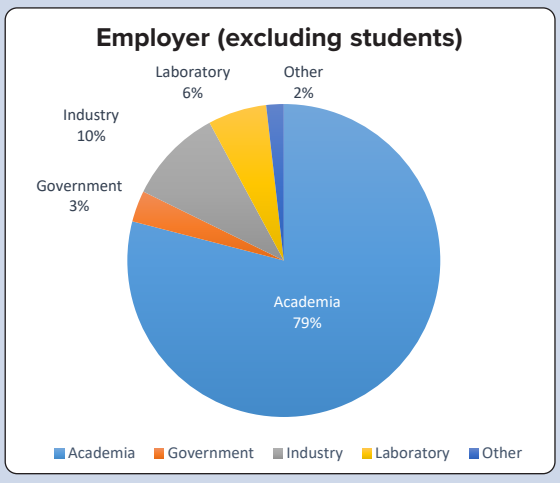

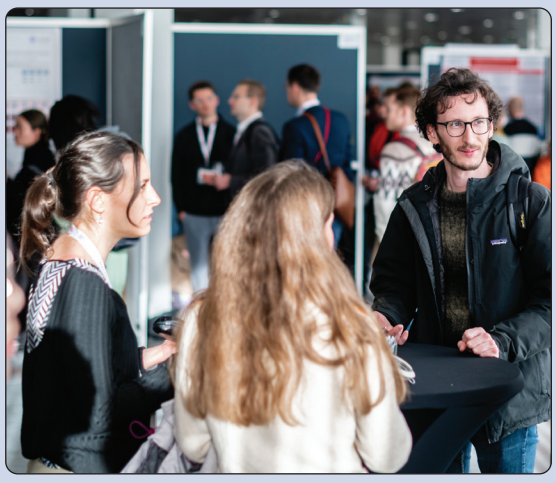

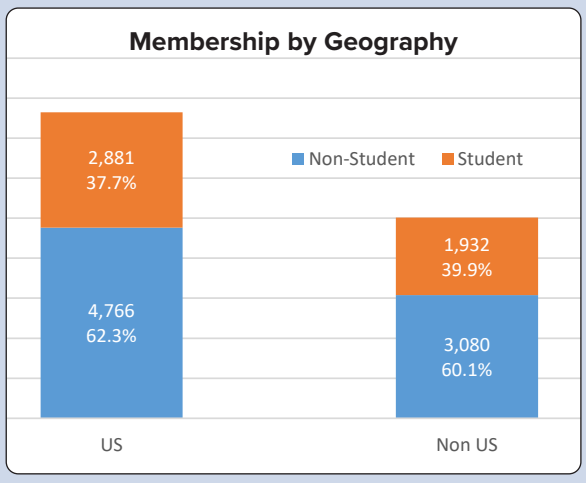

When You Renew Your SIAM Membership This Fall...

Please consider checking the "auto-renew" box to have your membership automatically renew at the end of 2024. You can update or cancel your auto-renewal information and preferences any time at ***my.siam.org.***

SIAM-Simons Undergraduate Summer Research Program Seeks Mentors

The program seeks mentors for the summer 2025 cycle. Funding covers food, lodging, travel, and stipend for participants and stipend for mentors. Applications to be a mentor for two students for eight weeks open in July and close at the end of August. Visit ***siam.org/simons*** for more information.

Nominate two of your students for free membership!

SIAM members (excluding student members) can nominate up to two students per year for free membership. Go to ***www.siam.org/Forms/Nominate-a-Student*** to make your nominations.

Nominations are open for the SIAM Fellows Class of 2025!

Support your profession by nominating up to two colleagues for excellence in research, industrial work, educational activities, or other activities related to the goals of SIAM. Class of 2025 Fellows nominations are being accepted at *nominatefellows.siam.org* until October 18, 2024.

siam. Fellow

FOR MORE INFORMATION ON SIAM MEMBERSHIP: ***siam.org/membership***

siam | BOOKS

Quality and Value in Mathematical Science Literature

Look for These Books and Others at SIAM's Summer Conferences

Algorithmic Mathematics in Machine Learning

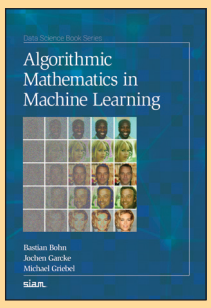

Bastian Bohn, Jochen Garcke, and Michael Griebel

This unique book explores several well-known machine learning and data analysis algorithms from a mathematical and programming perspective. The authors present machine learning methods, review the underlying mathematics, and provide programming exercises to deepen the reader's understanding. They provide new terminology and background information on mathematical concepts, as well as exercises, in "info-boxes" throughout the text. Application areas are accompanied by exercises that explore the unique characteristics of real-world data sets.

2024 / xii + 225 pages / Softcover / 978-1-61197-787-5 / List $64.00 / SIAM Member $44.80 / DI03

Handbook of Writing for the Mathematical Sciences
Third Edition

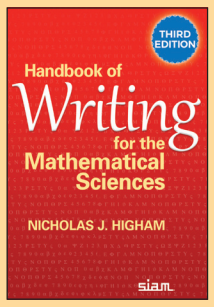

Nicholas J. Higham

This third edition revises, updates, and expands the best-selling second edition to reflect modern writing and publishing practices and builds on the author's extensive experience in writing and speaking about mathematics.

2019 / xxii + 353 pages / Softcover / 978-1-611976-09-0
List $71.50 / SIAM Member $50.05 / Student $34.50
OT167

A Toolbox for Digital Twins
From Model-Based to Data-Driven

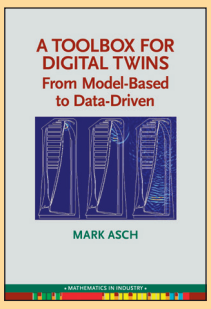

Mark Asch

This book brings together the mathematical and numerical frameworks needed for developing digital twins. Starting from the basics and moving on to data assimilation, inverse problems, and Bayesian uncertainty quantification, the book provides a comprehensive toolbox for digital twins. Emphasis is also placed on the design process, denoted as the "inference cycle," the aim of which is to propose a global methodology for complex problems.

2022 / xxiv + 832 pages / Softcover / 978-1-611976-96-0 / List $120.00 / SIAM Member $84.00 / MN06

How to Be Creative
A Practical Guide for the Mathematical Sciences

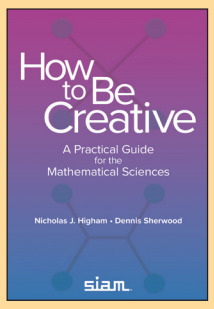

Nicholas J. Higham

Do you know precisely how your creativity happens? Can you coach other people to be more creative? This book is a how-to guide focused on helping people working in the mathematical sciences to generate great—or even greater—ideas by showing them "how to do it" and how to teach others how to do it, too. It provides a proven process for idea generation and a wide range of mathematically oriented examples.

2022 / xii + 109 pages / Softcover / 978-1-611977-02-8
List $29.00 / SIAM Member $20.30 / OT179

Introduction to Nonlinear Optimization
Theory, Algorithms, and Applications with Python and MATLAB, Second Edition

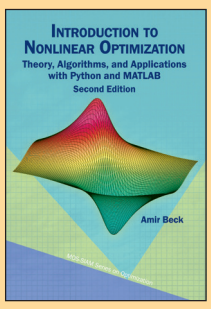

Amir Beck

Built on the framework of the successful first edition, this book serves as a modern introduction to the field of optimization. The author provides the foundations of theory and algorithms of nonlinear optimization and presents a variety of applications from diverse areas of applied sciences. The book gradually yet rigorously builds the connections between theory, algorithms, applications, and actual implementation and contains several topics not typically included in optimization books.

2023 / xii + 354 / softcover / 978-1-61197-761-5 / List $84.00 / SIAM Member $58.80 / MO32

BIG Jobs Guide
Business, Industry, and Government Careers for Mathematical Scientists, Statisticians, and Operations Researchers

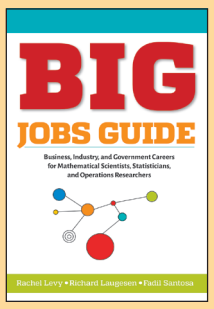

Rachel Levy, Richard Laugesen, and Fadil Santosa

Jobs using mathematics, statistics, and operations research are projected to grow by almost 30% over the next decade. *BIG Jobs Guide* helps job seekers at every stage of their careers in these fields explore opportunities in business, industry, and government (BIG) by providing insight on topics such as what skills to offer employers, how to write a high-impact resumé, where to find a rewarding internship, and what kinds of jobs are out there.

2018 / xii + 141 pages / Softcover / 978-1-611975-28-4
List $28.00 / SIAM Member $19.60 / Student $15.00
OT158

Numerical Linear Algebra with Julia

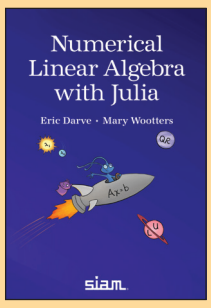

Eric Darve and Mary Wootters

This book provides in-depth coverage of fundamental topics in numerical linear algebra, including how to solve dense and sparse linear systems, compute QR factorizations, compute the eigendecomposition of a matrix, and solve linear systems using iterative methods such as conjugate gradient. It contains detailed descriptions of algorithms along with illustrations and graphics that emphasize core concepts and demonstrate the algorithms. Julia code is provided to illustrate concepts and allow readers to explore methods on their own.

2021 / xiv + 406 pages / Softcover / 978-1-611976-54-0 / List $89.00 / SIAM Member $62.30 / OT172

Computed Tomography
Algorithms, Insight, and Just Enough Theory

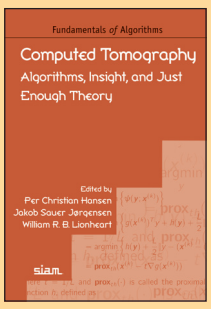

Edited by Per Christian Hansen, Jakob Sauer Jørgensen, and William R. B. Lionheart

This book describes fundamental computational methods for image reconstruction in computed tomography (CT) with a focus on a pedagogical presentation of these methods and their underlying concepts. Insights into the advantages, limitations, and theoretical and computational aspects of the methods are included, giving a balanced presentation that allows readers to understand and implement CT reconstruction algorithms.

2021 / xviii + 337 pages / Softcover / 978-1-611976-66-3 / List $89.00 / SIAM Member $62.30 / FA18

Scientific Computing
An Introductory Survey, Revised Second Edition

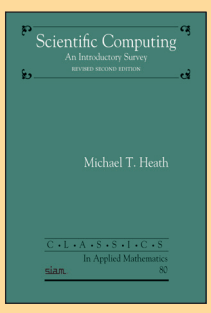

Michael T. Heath

This book presents a broad overview of methods and software for solving mathematical problems arising in computational modeling and data analysis, including proper problem formulation, selection of effective solution algorithms, and interpretation of results. Its focus is on the motivation and ideas behind the algorithms presented.

2018 / xx + 567 pages / Softcover / 978-1-611975-57-4 / List $100.00 / SIAM Member $70.00 / CL80

Order online: *bookstore.siam.org*

Or call toll-free in U.S. and Canada:
800-447-SIAM; worldwide: +1-215-382-9800

If you live outside North or South America, order from *eurospanbookstore.com/siam* for speedier service.
Eurospan honors the SIAM member discount.
Contact customer service (*service@siam.org*) for the code to use when ordering.

FOR MORE INFORMATION ON SIAM BOOKS: ***siam.org/books***

siam | JOURNALS

Where You Go to Know and Be Known

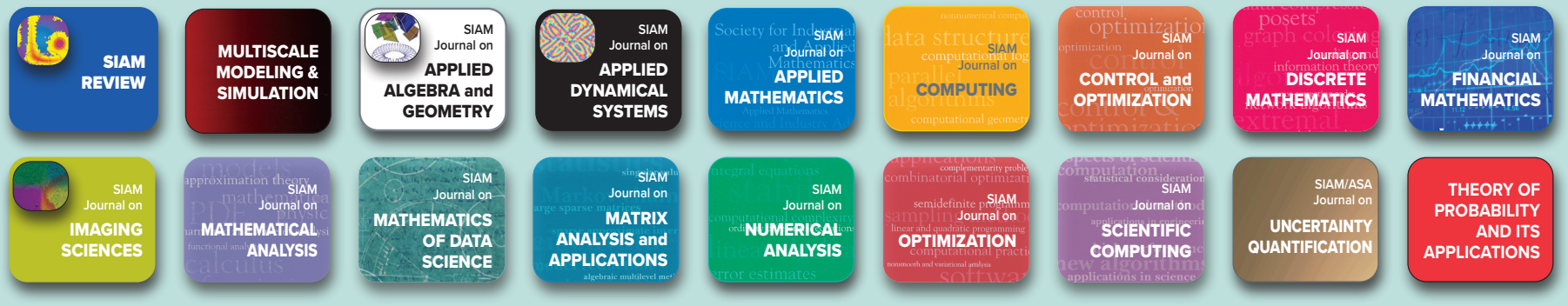

Recently Posted Articles

MULTISCALE MODELING & SIMULATION: A SIAM Interdisciplinary Journal

On the Nature of the Boundary Resonance Error in Numerical Homogenization and Its Reduction
Sean P. Carney, Milica Dussinger, and Björn Engquist

Topological Sensitivity-Based Analysis and Optimization of Microstructured Interfaces
Marie Touboul, Rémi Cornaggia, and Cédric Bellis

Boundary Homogenization for Partially Reactive Patches
Claire E. Plunkett and Sean D. Lawley

SIAM Journal on APPLIED ALGEBRA and GEOMETRY

Explicit Non-special Divisors of Small Degree, Algebraic Geometric Hulls, and LCD Codes from Kummer Extensions
Eduardo Camps Moreno, Hiram H. López, and Gretchen L. Matthews

Decomposable Context-Specific Models
Yulia Alexandr, Eliana Duarte, and Julian Vill

Function Space and Critical Points of Linear Convolutional Networks
Kathlén Kohn, Guido Montúfar, Vahid Shahverdi, and Matthew Trager

SIAM Journal on APPLIED DYNAMICAL SYSTEMS

On Higher Order Drift and Diffusion Estimates for Stochastic SINDy
Mathias Wanner and Igor Mezić

***N*-Body Oscillator Interactions of Higher-Order Coupling Functions**
Youngmin Park and Dan Wilson

Emergence of Polarization in a Sigmoidal Bounded-Confidence Model of Opinion Dynamics
Heather Z. Brooks, Philip S. Chodrow, and Mason A. Porter

SIAM Journal on APPLIED MATHEMATICS

Exact Power Spectrum in a Minimal Hybrid Model of Stochastic Gene Expression Oscillations
Chen Jia, Hong Qian, and Michael Q. Zhang

A Stabilizing Effect of Advection on Planar Interfaces in Singularly Perturbed Reaction-Diffusion Equations
Paul Carter

Longitudinal Shear Flow over a Superhydrophobic Grating with Partially Invaded Grooves and Curved Menisci
Ehud Yariv

SIAM Journal on COMPUTING

AdWords in a Panorama
Zhiyi Huang, Qiankun Zhang, and Yuhao Zhang

Rapid Mixing of Glauber Dynamics via Spectral Independence for All Degrees
Xiaoyu Chen, Weiming Feng, Yitong Yin, and Xinyuan Zhang

Semialgebraic Proofs, IPS Lower Bounds, and the τ-Conjecture: Can a Natural Number Be Negative?
Yaroslav Alekseev, Dima Grigoriev, Edward A. Hirsch, and Iddo Tzameret

SIAM Journal on CONTROL and OPTIMIZATION

Global Uniform Finite-Time Output Feedback Stabilization for Disturbed Nonlinear Uncertain Systems: Backstepping-Like Observer and Nonseparation Principle Design
Wenwu Zhu and Haibo Du

Mean Field Games in a Stackelberg Problem with an Informed Major Player
Philippe Bergault, Pierre Cardaliaguet, and Catherine Rainer

Distributed Global Consensus of LTI Mass with Heterogeneous Actuator Saturation and Communication Noises
Xiaoling Wang, Juan Qian, Housheng Su, Xiujuan Lu, and James Lam

SIAM Journal on DISCRETE MATHEMATICS

On the Minimum Number of Arcs in *k*-Dicritical Oriented Graphs
Pierre Aboulker, Thomas Bellitto, Frédéric Havet, and Clément Rambaud

On Graphs Coverable by *k* Shortest Paths
Maël Dumas, Florent Foucaud, Anthony Perez, and Ioan Todinca

Brillouin Zones of Integer Lattices and Their Perturbations
Herbert Edelsbrunner, Alexey Garber, Mohadese Ghafari, Teresa Heiss, Morteza Saghafian, and Mathijs Wintraecken

SIAM Journal on FINANCIAL MATHEMATICS

Nonasymptotic Estimation of Risk Measures Using Stochastic Gradient Langevin Dynamics
Jiarui Chu and Ludovic Tangpi

Risk Measures beyond Frictionless Markets
Maria Arduca and Cosimo Munari

Optimal Clearing Payments in a Financial Contagion Model
Giuseppe C. Calafiore, Giulia Fracastoro, and Anton V. Proskurnikov

SIAM Journal on IMAGING SCIENCES

Stable Local-Smooth Principal Component Pursuit
Jiangjun Peng, Hailin Wang, Xiangyong Cao, Xixi Jia, Hongying Zhang, and Deyu Meng

Extrapolated Plug-and-Play Three-Operator Splitting Methods for Nonconvex Optimization with Applications to Image Restoration
Zhongming Wu, Chaoyan Huang, and Tieyong Zeng

Stochastic Variance Reduced Gradient for Affine Rank Minimization Problem
Ningning Han, Juan Nie, Jian Lu, and Michael K. Ng

SIAM Journal on MATHEMATICAL ANALYSIS

Uniform Far-Field Asymptotics of the Two-Layered Green Function in Two Dimensions and Application to Wave Scattering in a Two-Layered Medium
Long Li, Jiansheng Yang, Bo Zhang, and Haiwen Zhang

Nonlocal Problems with Local Boundary Conditions I: Function Spaces and Variational Principles
James M. Scott and Qiang Du

Generalized Impedance Boundary Conditions with Vanishing or Sign-Changing Impedance
Laurent Bourgeois and Lucas Chesnel

SIAM Journal on MATHEMATICS of DATA SCIENCE

The Geometric Median and Applications to Robust Mean Estimation
Stanislav Minsker and Nate Strawn

Scalable Tensor Methods for Nonuniform Hypergraphs
Sinan G. Aksoy, Ilya Amburg, and Stephen J. Young

Robust and Tuning-Free Sparse Linear Regression via Square-Root Slope
Stanislav Minsker, Mohamed Ndaoud, and Lang Wang

SIAM Journal on MATRIX ANALYSIS and APPLICATIONS

Preconditioner Design via Bregman Divergences
Andreas A. Bock and Martin S. Andersen

A Skew-Symmetric Lanczos Bidiagonalization Method for Computing Several Extremal Eigenpairs of a Large Skew-Symmetric Matrix
Jinzhi Huang and Zhongxiao Jia

Differential Geometry with Extreme Eigenvalues in the Positive Semidefinite Cone
Cyrus Mostajeran, Nathaël Da Costa, Graham Van Goffrier, and Rodolphe Sepulchre

SIAM Journal on NUMERICAL ANALYSIS

A Finite Element Method for Hyperbolic Metamaterials with Applications for Hyperlens
Fuhao Liu, Wei Yang, and Jichun Li

The (*p*, *p* – 1)-HDG Method for the Helmholtz Equation with Large Wave Number
Bingxin Zhu and Haijun Wu

Inverse Wave-Number-Dependent Source Problems for the Helmholtz Equation
Hongxia Guo and Guanghui Hu

SIAM Journal on OPTIMIZATION

Parameter-Free Accelerated Gradient Descent for Nonconvex Minimization
Naoki Marumo and Akiko Takeda

Approximation Guarantees for Min-Max-Min Robust Optimization and *k*-Adaptability under Objective Uncertainty
Jannis Kurtz

Stochastic Trust-Region and Direct-Search Methods: A Weak Tail Bound Condition and Reduced Sample Sizing
F. Rinaldi, L. N. Vicente, and D. Zeffiro

SIAM Journal on SCIENTIFIC COMPUTING

Spectral Analysis of Implicit *s*-Stage Block Runge–Kutta Preconditioners
Martin J. Gander and Michal Outrata

A New Locally Divergence-Free Path-Conservative Central-Upwind Scheme for Ideal and Shallow Water Magnetohydrodynamics
Alina Chertock, Alexander Kurganov, Michael Redle, and Kailiang Wu

The Numerical Flow Iteration for the Vlasov–Poisson Equation
Matthias Kirchhart and R. Paul Wilhelm

SIAM/ASA Journal on UNCERTAINTY QUANTIFICATION

One-Shot Learning of Surrogates in PDE-Constrained Optimization under Uncertainty
Philipp A. Guth, Claudia Schillings, and Simon Weissmann

Computationally Efficient Sampling Methods for Sparsity Promoting Hierarchical Bayesian Models
D. Calvetti and E. Somersalo

Differential Equation–Constrained Optimization with Stochasticity
Qin Li, Li Wang, and Yunan Yang